Interannual variability in the ecosystem CO_2 fluxes at a paludified spruce forest and ombrotrophic bog in the southern taiga

Vadim Mamkin[1,2]**, Vitaly Avilov**[1]**, Dmitry Ivanov**[1]**, Andrey Varlagin**[1]**, and Julia Kurbatova**[1]

[1]A. N. Severtsov Institute of Ecology and Evolution, Russian Academy of Sciences,
33 Leninsky Avenue, 119071 Moscow, Russia
[2]Faculty of Geography and Geoinformation Technology, National Research University Higher School of
Economics, 11 Pokrovsky Bulvar, 109028 Moscow, Russia

Correspondence: Vadim Mamkin (vadimmamkin@gmail.com)

Abstract. Climate warming in high latitudes impacts CO_2 sequestration of the northern peatlands through the changes in production and decomposition processes. The response of the net CO_2 fluxes between ecosystems and the atmosphere to climate change and weather anomalies can vary across forest and non-forest peatlands. To better understand the differences in CO_2 dynamics at forest and non-forest boreal peatlands induced by changes in environmental conditions, the estimates of interannual variability in the net ecosystem exchange (NEE), total ecosystem respiration (TER), and gross primary production (GPP) was obtained at two widespread peatland ecosystems – paludified spruce forest and the adjacent ombrotrophic bog in the southern taiga of west Russia using 6 years of paired eddy covariance flux measurements. Both positive and negative annual and growing season air temperature and precipitation anomalies were observed in the period of measurement (2015–2020). Flux measurements showed that, in spite of the lower growing season TER ($332 \pm 17 \ldots 339 \pm 15\,\mathrm{gC\,m^{-2}}$) and GPP ($442 \pm 13 \ldots 464 \pm 11\,\mathrm{gC\,m^{-2}}$) rates, the bog had a higher CO_2 uptake rates (NEE was $-132 \pm 11 \ldots -108 \pm 6$) than the forest, except for the warmest and the wettest year of the period (2020), and was an atmospheric CO_2 sink in the selected years, while the forest was a CO_2 sink or source, depending on the environmental conditions. Growing season NEE at the forest site was between -142 ± 48 and $28 \pm 40\,\mathrm{gC\,m^{-2}}$, TER between 1135 ± 64 and $1366 \pm 58\,\mathrm{gC\,m^{-2}}$, and GPP between 1207 ± 66 and $1462 \pm 107\,\mathrm{gC\,m^{-2}}$. Annual NEE at the forest was between -62 ± 49 and $145 \pm 41\,\mathrm{gC\,m^{-2}}$, TER between 1429 ± 87 and $1652 \pm 44\,\mathrm{C\,m^{-2}}$, and GPP between 1345 ± 89 and $1566 \pm 41\,\mathrm{gC\,m^{-2}}$, respectively. Under the anomalously warm winter conditions with sparse and thin snow cover (2019/2020), the increased daily GPP, TER, and net CO_2 uptake at the forest was observed, while at the bog, the changes in CO_2 fluxes between the warm and cold winters were not significant. This study suggests that the warming in winter can increase the CO_2 uptake of the paludified spruce forests of the southern taiga in non-growing seasons.

1 Introduction

The CO_2 net ecosystem exchange (NEE) between peatlands and the atmosphere is an important process of the global carbon cycle, controlling the terrestrial carbon stocks and influencing the climate system (Gorham, 1991; Aurela et al., 2002; Wieder and Vitt, 2006). Northern peatlands store about 500 ± 100 Gt of C (Yu, 2012), which is approximately equal to the global vegetation and about 20%–30% of the soil carbon stocks (Friedlingstein et al., 2019). Annual CO_2 uptake of the peatlands in high latitudes is relatively small (Moore, 2002; Koehler et al., 2011) due to the low productivity and decomposition rates limited by wet anoxic conditions, low temperatures, and pH, as well as low nitrogen content, in the peat (Wieder and Vitt, 2006; Weedon et al., 2013). However, northern peatlands are considered to be a stable sink of atmospheric CO_2 at the long timescales (Gorham, 1991; Moore, 2002; Alexandrov et al., 2020), as the carbon accumulation from gross primary production (GPP) exceeds carbon loss through CO_2 release from total ecosystem respiration total ecosystem respiration (TER) and from the other mechanisms, i.e. methane emissions and dissolved organic carbon (DOC) runoff.

A warming trend in high latitudes is able to intensify both the carbon accumulation and release processes affecting the NEE and net ecosystem carbon balance of the northern peatlands (Loisel et al., 2021). It is suggested that growing air and peat temperatures, especially under the rising frequency of droughts in boreal regions, can significantly increase decomposition rates and switch peatlands from CO_2 sinks to CO_2 sources for the atmosphere (e.g. Alm et al., 1999; Moore, 2002; Lund et al., 2012; LaFleur et al., 2015; Helbig et al., 2019; Loisel et al., 2021).

The response of the peatlands to climate change and weather anomalies may differ across the ecosystems, depending on peatland type, local weather, and hydrological regime, as well as vegetation composition and management practices (Humphreys et al., 2006; Euskirchen et al., 2014; Petrescu et al., 2015; Holl et al., 2020; Qiu et al., 2020). In recent decades, numerous experimental studies have shown a high spatial and temporal variability in the CO_2 fluxes between different peatland ecosystems in high latitudes and its response to environmental factors (e.g. Alm et al., 1999; Humphreys et al., 2006; Lindroth et al., 2007; Minkkinen et al., 2018; Park et al., 2021). Previous studies reported that the NEE of the peatlands is susceptible to water table depth (WTD) dynamics, air and peat temperature variations, changes in global radiation, and the timing of the snow-melting and peat layer thaw (Moore, 2002; Dunn et al., 2007; Lindroth et al., 2007; Sulman et al., 2010).

Forest and non-forest peatlands have a different features which determine the ecosystem–atmosphere carbon dioxide exchange, i.e. aboveground biomass, peat thickness, nutrient availability, and the different temperature and moisture regime of the upper peat layer (Moore, 2002; Kurbatova et al., 2013; Euskirchen et al., 2014; Beaulne et al., 2021). At short timescales, the forest peatlands (i.e. paludified forests) can have similar carbon accumulation rates to the non-forest peatlands (i.e. bogs), but the forest peatlands have a lower CO_2 sequestration rates at long timescales (Beaulne et al., 2021). Moreover, the NEEs of the forest and non-forest peatlands have their own seasonal specifics. For instance, the forest peatlands can sequestrate atmospheric CO_2 before the snow-melting and peat thaw in spring, while a thawing is necessary for the beginning of the CO_2 uptake at non-forest peatlands (Tanja et al., 2003; Euskirchen et al., 2014; Helbig et al., 2019). Therefore, the changes in the environmental conditions can influence the CO_2 fluxes at the forest and non-forest peatlands in different ways. With regard to the strong dependence of NEE on the environmental parameters of variability, regional and site-specific features of the peatlands, and its significant potential feedbacks to the climate system in response to the global warming (IPCC, 2014; Helbig et al., 2020; Loisel et al., 2021), the experimental estimates of the interannual variability in the ecosystem CO_2 fluxes at different peatlands located in the same landscape are very useful for assessing the diversity of the possible effects of the weather anomalies and climate change on the ecosystem carbon dioxide exchange between the northern peatlands and the atmosphere (Lavoie et al., 2005; Ueyama et al., 2014; Park et al., 2021).

Unfortunately, in spite of numerous experimental studies focused on ecosystem–atmosphere CO_2 fluxes in different peatland types in high latitudes in North America (e.g. Roulet et al., 2007; Gill et al., 2017), Europe (e.g. Kurbatova et al., 2002; Lindroth et al., 2007; Minkkinen et al., 2018), and Asia (e.g. Tchebakova et al., 2015; Alekseychik et al., 2017; Park et al., 2021), there is lack of studies considering the ecosystem CO_2 fluxes at the forest and non-forest peatlands located in the same landscape and undergoing the similar weather conditions (e.g. Euskirchen et al., 2014; Helbig et al., 2017; Zagirova et al., 2019).

Russian peatlands cover about one-third of the global peatland area (Vompersky et al., 2011). Approximately 15% of forest and non-forest peatlands in Russia are located in the European part of the country and belong to the most widespread ecosystems in western Russia (Vompersky et al., 2011). However, the ecosystem flux data collected at peatlands in European Russia and available in the literature (e.g. Kurbatova et al., 2002, 2008; Zagirova et al., 2019) are very sparse and rarely cover a few years of measurements, which confines the research of the dependence between CO_2 fluxes and environmental conditions to interannual timescales.

This study is focused on CO_2 peatland–atmosphere exchange at two widespread ecosystem types in western Russia – an ombrotrophic bog and a paludified spruce forest located in western part of the Valdai Hills. The aim of the study was to analyse the interannual variability in NEE, TER, and GPP at the ombrotrophic bog and the paludified spruce forest lo-

cated in the same landscape and to establish the response of CO_2 fluxes to the interannual variability in environmental conditions using 6 years of paired eddy covariance flux measurements.

2 Methods

2.1 Study sites

This study was conducted at a paludified spruce forest (56.4615° N, 32.9221° E, 265 m a.s.l., above sea level) and adjacent ombrotrophic bog (56.4727° N, 33.0413° E, 240 m a.s.l.) located on the territory of the Central Forest State Nature Biosphere Reserve (CFSNBR) in the southwestern part of the Valdai Hills in the Tver region of Russia (Fig. 1a). The sites are located 7.5 km apart (Fig. 1b) and characterized by very similar weather conditions.

The study area belongs to a humid continental climate (Dfb type in the Köppen–Geiger climate classification; Kuricheva et al., 2017; Peel et al., 2007). According to the meteorological station Toropets (56.48° N, 31.63° E, 187 m a.s.l.), which is located 80 km west of the reserve, the mean air temperature at 2 m height for the period 1991–2020 was 5.7 °C (−5.9 °C in January and 18.2 °C in July). Long-term mean annual precipitation (1991–2020) measured at meteorological station Lesnoy Zapovednik (56.50° N, 32.83° E, 240 m a.s.l.) – the nearest meteorological station to the study area – was 778 mm (continuous air temperature data from Lesnoy Zapovednik meteostation for the 1991–2020 period are not available). Soil surface is typically covered by snow from mid-November to late March–early April (Desherevskaya et al., 2010), and the growing season is calculated as the number of days between the first 5 d period with mean daily air temperatures above 5 °C (start of the growing season) to the first 5 d period with mean daily air temperatures below 5 °C (end of the growing season; following Urban SIS, 2018; Buitenwerf et al., 2015; Donat et al., 2013; Mueller et al., 2015), which lasts 182 d on average (from 12 April to 11 October). Annual precipitation in the study region exceeds the potential evapotranspiration (PET) that determines excessive moistening conditions (Mamkin et al., 2019). The climate moisture index (CMI), calculated as the ratio of annual precipitation to annual potential evapotranspiration and which ranges between −1 and 1 (Wilmott and Feddema, 1992), is 0.3–0.4 (Novenko and Olchev, 2015; Mamkin et al., 2019). In the last 30 years, a positive trend of air temperature (+0.73 °C per 10 years) and precipitation (+3.6 mm per month per 10 years) has been detected at the meteorological stations Toropets and Lesnoy Zapovednik, respectively.

The vegetation of the reserve is represented by typical plant communities of the southern taiga, which are widespread at the plains in the northern part of Eastern Europe (Mamkin et al., 2019; Schulze et al., 2002; Vygodskaya et al., 2002). Excessive moistening coupled with

spread of glacial clay soils in the territory make the study area favourable to paludification processes and peat formation. Large areas of the CFSNBR are covered by fens, bogs, and paludified forests (Schulze et al., 2002; Puzachenko et al., 2014).

The paludified spruce forest (PF), named RU-Fyo in the FLUXNET database, is located in a shallow depression (Kurbatova et al., 2013) on peaty podzolic gley soils. PF is an old (with tree ages up to 200 years) forest with Norway spruce (*Picea abies* – 86 %) and white birch (*Betula pubescens* – 14 %) and an undergrowth dominated by Girgensohn's sphagnum (*Sphagnum girgensohnii* L.) and blueberry (*Vaccinium myrtillus* Russ.; Milyukova et al., 2002; Kurbatova et al., 2008; Kuricheva et al., 2017). The mean tree height is 16.9 ± 6.4 m ($\pm$ SD), with a mean diameter at breast height (DBH) of 21.6 ± 8.9 cm ($\pm$ SD), and the undergrowth is about 0.3 m. The average leaf area index (LAI) at the PF site is 3.5. The thickness of the peat layer at the site is 60 cm, with most of the root biomass at a depth of about 30 cm. The groundwater table is usually close to the surface. Peat soils have a poor soil aeration, low pH (3.5–3.8), and a low nitrogen content (0.5–9.9 kg ha^{-1}; Kurbatova et al., 2013; Milyukova et al., 2002; Vygodskaya et al., 2002).

The Staroselsky Mokh site (OB), named RU-Fy4 in FLUXNET database, is an old (up to 9000 years) ombrotrophic bog with an area of about 6 km^2 (Ivanov et al., 2021). The bog's vegetation is represented by different plant communities associated with topography microforms (i.a. ridges, hummocks, and hollows). The vegetation of the ridges and hummocks is dominated by different herbaceous species, including *Drosera rotundifolia* L., *Rhynchospora alba* (L.) Vahl., and *Eriophorum vaginatum* L., shrubs, including *Chamaedaphne calyculata* (L.) Moench, *Andromeda polifolia* L., *Rhododendron tomentosum* Harmaja, and *Vaccinium oxycoccos* L., and mosses, including *Sphagnum fuscum* (Schimp.) H. Klinggr., *S. medium* Limpr., and *S. angustifolium* (C. E. O. Jensen ex Russow) C. E. O. Jensen. The vegetation of hollows is dominated by herbs, including *Scheuchzeria palustris* L., *Rhynchospora alba* (L.) Vahl., *Carex limosa* L., *Drosera anglica* Huds., and *Eriophorum vaginatum* L., and mosses, including *Sphagnum fallax* (H. Klinggr.) H. Klinggr., *S. majus* (Russow) C. E. O. Jensen, *S. cuspidatum* Ehrh. ex Hoffm., *S. balticum* (Russow) C. E. O. Jensen, *Odontoschisma fluitans* (Nees) L. Söderstr. and Váňa, and *Gymnocolea inflata* (Huds.) Dumort. (Ivanov et al., 2021). The bog edges are covered by trees, predominantly by Scots pine (*Pinus sylvestris*), with tree heights up to 10–13 m. In the central part of the bog, small pine trees (within 2–5 m height) grow on some ridges.

The average peat layer thickness at the OB site is 3.2 m, with a maximum of 5.5 m (Ivanov et al., 2021). The groundwater level is typically 30 cm below the surface at ridges and hummocks and 10 cm above the surface at hollows.
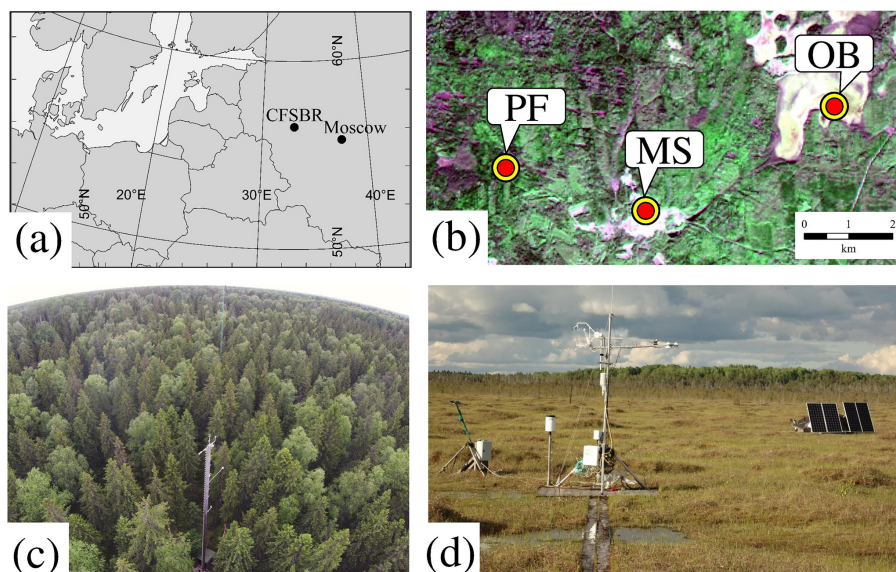
Figure 1. (a) Geographical location of the Central Forest State Nature Biosphere Reserve (CFSNBR). **(b)** Location of the paludified spruce forest (PF), ombrotrophic bog Staroselsky Mokh (OB), and meteorological station Lesnoy Zapovednik (MS) on a Landsat 8 image. Photos of the eddy covariance stations at the **(c)** PF and **(d)** OB sites.

2.2 Measurements

Flux stations at the PF and OB sites have a standard instrumentation for the FLUXNET network. Flux measurements at the PF site started in 1998 (Kurbatova et al., 2013). Eddy covariance instruments are mounted on the top of a 29 m tower located in the central part of the ecosystem (Fig. 1c). Flux measurements were obtained using 3-D sonic anemometer (Gill Solent R3; Gill Instruments Limited, UK) and a closed-path CO_2/H_2O gas analyser (LI-6262-3; LI-COR Inc., USA). Eddy covariance data were collected on a flash drive, using a personal computer with EDDYMEAS data acquisition software (Kolle and Rebmann, 2007). Global radiation was measured using a radiometer, Kipp & Zonen CNR4 (OTT HydroMet B. V., the Netherlands), at 28 m height. Air temperature and relative humidity measurements were carried out at 28 m height using a humidity and temperature probe (HMP35D; Vaisala, Finland) and atmospheric pressure measurement device (PTB101B; Vaisala, Finland) at the same height. Precipitation was measured using tipping-bucket rain gauge (52202H; R. M. Young Company, USA) at 20 m height. WTD was measured using a pressure transducer (CS451; Campbell Scientific, Inc., USA), at 1.8 m depth. Soil temperature measurements at 5 cm depth were obtained using three reflectometers (CS650; Campbell Scientific, Inc., USA). Meteorological data were collected every 10 s using a data logger (DL3000; Delta-T Devices Ltd, UK).

Eddy covariance and meteorological instruments at the OB site were installed in 2015 on a 3.5 m tripod which was placed in the central part of the bog (Fig. 1d). Instruments for flux measurements included a 3-D sonic anemometer (CSAT3; Campbell Scientific, Inc., USA) and open-path CO_2/H_2O gas analyser (LI-7500A; LI-COR Inc., USA) mounted at 2.85 m height. Eddy covariance data were collected using LI-7550 analyser interface unit (LI-COR Inc., USA) at a frequency of 10 Hz.

Additionally, global radiation at the OB site was measured with a four-component radiometer (NR01; Hukseflux, the Netherlands) at 2.5 m height. Air temperature, relative humidity, and atmospheric pressure was measured using a weather transmitter (HMP155; Vaisala, Finland) at 2 m height. Precipitation was measured by a rain gauge Young 52202 (Young 52202; R. M. Young Company, USA) at 1 m height near the tripod. WTD measurements were obtained using a submersible pressure transducer (CS451; Campbell Scientific, Inc., USA) installed 1.67 m below the surface. The temperature of the peat layer at 5 cm depth was measured by three temperature probes (T109; Campbell Scientific, Inc., USA) placed in hollow, in hummock, and between them. Meteorological data were collected every 1 min using the data logger (CR1000; Campbell Scientific, Inc., USA). Moscow time (UTC+3) was used for data storage.

2.3 Data processing and statistical analysis

This study is based on eddy covariance and meteorological data obtained at the PF and OB sites in 2015–2020. Net ecosystem exchange (NEE) at two sites was calculated for 30 min intervals using EddyPro software (LI-COR Inc., USA) with all required statistical tests and corrections. The footprint was estimated using the Kljun et al. (2004) model. In total, 0–2 quality flags (Mauder and Foken, 2006) were as-

signed to the calculated fluxes. All fluxes with quality flag 2 were removed from the analysis following the recommendations of the data quality assessment (Mauder et al., 2013). Additionally, all data containing spikes, from having been collected under rain and dew events and under low turbulence, were also filtered out. Storage terms were calculated using the one-point approach (Greco and Baldocchi, 1996) and added to CO$_2$ flux values. u^* filtering of NEE, gap-filling, and NEE partitioning into GPP and TER was carried out using the REddyProc package (Wutzler et al., 2018).

The mean annual u^* threshold for NEE at the PF site varied between 0.354 and 0.529 m s^{-1} and between 0.058 and 0.064 m s^{-1} at the OB site. Uncertainty in NEE, TER, and GPP associated with the random error in the measured fluxes, u^* threshold estimation, gap-filling, and flux partitioning procedures was calculated using the REddyProc package (Wutzler et al., 2018) as a standard deviation (SD) of the flux values. The aggregated random uncertainty in the seasonal and annual sums of the CO$_2$ fluxes was obtained considering the autocorrelation between the residuals using empirical autocorrelation function (Zięba and Ramza, 2011).

The statistical significance of the changes in the CO$_2$ fluxes between the years of measurements at the PF and OB sites was estimated using a Mann–Whitney U test (M–W U test) and Kruskal–Wallis analysis of variance (ANOVA; K–W test) with Dunn's post hoc test, as the daily TER, GPP, and NEE values were not normally distributed (Shapiro–Wilk test; $p < 0.05$).

2.4 Parameterization the dependence of CO$_2$ fluxes on environmental factors

The main ambient factors controlling CO$_2$ fluxes at the terrestrial ecosystems under the absence of water stress are soil and air temperatures and the global radiation (R_g). To research how TER and GPP rates varied following the changes in the environmental conditions, we considered the dependence of the nighttime TER on soil and air temperature and dependence of GPP on R_g. Only original NEE data were used for the calculation of TER and GPP for this analysis. To describe the dependence of TER on air and soil temperature, a widely used Q_{10} function was implemented. Q_{10} and R_{10} coefficients were calculated following Pavelka et al. (2007):

$$Q_{10} = \exp(10 \cdot \alpha), \qquad (1)$$

where α is an empirical parameter taken from

$$\ln(\text{TER}) = \alpha \cdot T + \gamma, \qquad (2)$$

where T is soil or air temperature (°C), and γ is an empirical parameter of the equation.

The dependence between GPP and R_g (W m^{-2}) was described using the well-known Michaelis–Menten hyperbolic light response curve:

$$\text{GPP} = \frac{\alpha \cdot \beta \cdot R_g}{\alpha \cdot R_g + \beta}, \qquad (3)$$

where α and β are the empirical parameters of the equation. α is a canopy light utilization parameter (µmol J^{-1}), and β is the maximum CO$_2$ uptake at light saturation (µmol m^{-2} s^{-1}; Matthews et al., 2017).

2.5 Additional data

The analysis of the weather conditions in the period 2015–2020 and the calculation of the mean long-term values of the meteorological parameters are based on the data collected at the two meteorological stations. Mean air temperature data downloaded from the RIHMI-WDC (Research Institute of Hydrometeorological Information World Data Centre) database (http://aisori-m.meteo.ru, last access: 11 March 2022) (RIHMI-WDI database, 2022) measured at Toropets station was used. Only precipitation and snow cover data collected nearest to the site's meteorological station Lesnoy Zapovednik was used, considering the non-uniform spatial distribution of the precipitation in the region and the lack of air temperature data collected at Lesnoy Zapovednik station.

3 Results

3.1 Meteorological conditions

A total of 6 years of measurements showed a wide interannual variability in the meteorological conditions (Fig. 2). According to the data from the meteorological station Toropets, the mean annual air temperature in the period 2015–2020 was higher than the long-term mean value for the period 1991–2020 (Table 1), except 2017, when a mean annual air temperature anomaly was not observed. An analysis of the precipitation data from meteorological station Lesnoy Zapovednik showed that annual precipitation in 2015 and 2018 was lower than the mean long-term annual precipitation sum and higher in 2016, 2017, 2019, and 2020. Mean air temperature calculated for the long-term growing season period (LTGS; 12 April–11 October) was lower in 2015, 2017, and 2019 than the long-term mean for the same period and higher in 2016, 2018, and 2020. LTGS precipitation was lower in 2015 and 2018 and higher in 2016, 2017, 2019, and 2020. Growing season precipitation correlated with annual precipitation sums, but the proportion between them increased from 45 % in 2015 to 65 % in 2020.

Therefore, the environmental conditions in the selected years were notably different. The year 2017 was the coldest of the period, with the lowest global radiation and relatively high annual and growing season precipitation. In contrast, 2018 was relatively warm, with the highest global radiation and lowest annual and growing season precipitation. The warmest and the wettest year (and growing season) of the period was 2020.

All winters (November–March) in the selected period (2015–2020), except winter 2017/2018, were warmer in rela-

Table 1. Meteorological conditions in the period 2016–2020, with the mean annual air temperature (T_a), mean air temperature calculated for the long-term growing season (LTGS; 12 April–11 October; $T_{a,g.s.}$), and growing season length (GSL) at meteorological station Toropets. The annual sum of precipitation (Pr) and sum of precipitation calculated for the LTGS period ($Pr_{g.s.}$) at meteorological station Lesnoy Zapovednik (MS) and the long-term (1991–2020) mean values of T_a, $T_{a,g.s.}$, Pr, and $Pr_{g.s.}$, with standard deviations ($\pm$ SD), are shown. Annual sums of global radiation (R_g), mean annual soil temperature (T_s) at 5 cm depth, and mean annual water table depth at paludified forest (PF) are shown.

	2015	2016	2017	2018	2019	2020	Long term
T_a (°C)	6.8	5.8	5.7	6.0	7.0	7.6	5.7 ± 0.8
$T_{a,g.s.}$ (°C)	13.5	14.3	12.3	14.8	13.4	13.8	13.6 ± 0.8
GSL (d)	180	187	174	194	172	178	182
Pr (mm)	671	864	956	560	848	992	778 ± 123
$Pr_{g.s.}$ (mm)	300	479	562	343	492	640	445 ± 114
R_g (MJ m^{-2})	3592	3402	3249	3659	3456	3333	
T_s (°C)	9.0*	6.7	6.0	6.7	6.6	6.7	
WTD (m)	0.63	0.28	0.13	0.37	0.16	0.16	

* T_s was calculated for 3 July–31 December 2015.

Table 2. Mean air temperature in the winters (1 November–31 March) of 2015–2020 and the mean long-term value of air temperature at meteorological station Toropets (°C), with the standard deviation ($\pm$ SD).

2015/2016	2016/2017	2017/2018	2018/2019	2019/2020	Long term
−2.2	−3.0	−3.5	−2.4	1.3	-3.5 ± 1.9

tion to the long-term means, but the mean winter air temperatures were primarily negative (Table 2). A positive mean winter air temperature was observed in winter 2019/2020. Snow cover formed from late October to the beginning of January and was melting in April, with snow depth reaching 40 cm. In winter 2019/2020, snow cover was anomalously sparse and thin (0–10 cm) and was observed only from the first week of January to mid-February.

Soil temperature and water table depth dynamics at the sites were influenced by seasonal and interannual changes in the weather conditions. The mean annual soil temperature at 5 cm depth was higher at the OB site than at the PF site in the growing season of the each year, where the mean daily soil temperature in summer reached 22.9 °C, while at the PF site it did not exceed 13.5 °C. On the contrary, in winter, the soil temperature at the PF site was higher than at the OB site; the mean daily soil temperature in winter varied between 1 and 3 °C at the PF site, while it reached 0 °C at the OB site. The WTD at the sites had a seasonal variation, so the minimal values were very similar and observed after the snow-melting in the spring of each year (−0.20 m at OB and −0.16 m at PF). Then, the WTD usually increased in late August and September to 1.2 m at the PF site and to 0.15 m at the OB site. In spite of the difference in precipitation between the years, groundwater at the OB site was close to the surface when the WTD at the PF site increased in summer to its maximal values in the years with lower precipitation and was within 0.40–0.50 m in the relatively wet years.

3.2 Ecosystem CO_2 fluxes

Eddy covariance CO_2 flux measurements showed a wide seasonal and interannual variability connected with the changes in environmental conditions among the study period (2015–2020). During the 6 years of measurements, CO_2 uptake at the PF site tended to increase. PF was a CO_2 source in 2015, 2016, 2017, and 2019 and a CO_2 sink in 2018 and 2020 (Table 3). Annual sums of CO_2 at the OB site were obtained only for 2020, when OB was a stronger CO_2 sink than at the PF site, but the annual sums of GPP and TER were lower by 3.0–3.5 times, respectively. The mean annual GPP/TER ratio at the PF site varied between 0.85–1.04 in the period 2015–2020 and was 1.23 at the OB site in 2020. At the PF site, the mean GPP/TER ratio in 2020 was significantly higher than in the previous years (K–W test; $H = 37.508$; $n = 2192$; $p < 0.001$; post hoc Dunn's test $p < 0.05$). Moreover, the difference between the GPP/TER ratio in the other years was not significant. Maximal and minimal annual NEE, TER, and GPP at the PF site were not correspondent with maximal and minimal growing season length (GSL). Minimal values of annual GPP at the PF site were observed in the years with relatively low air temperatures (2016 and 2017), and the relatively high values of annual GPP corresponded to the years with high global radiation (2015, 2018, and 2019). Annual sums of TER at the PF site were minimal in the years with maximal precipitation and, correspondingly, with the minimal mean annual WTD. However, due to the high uncertainty in annual TER and GPP at the PF site, comparable with its
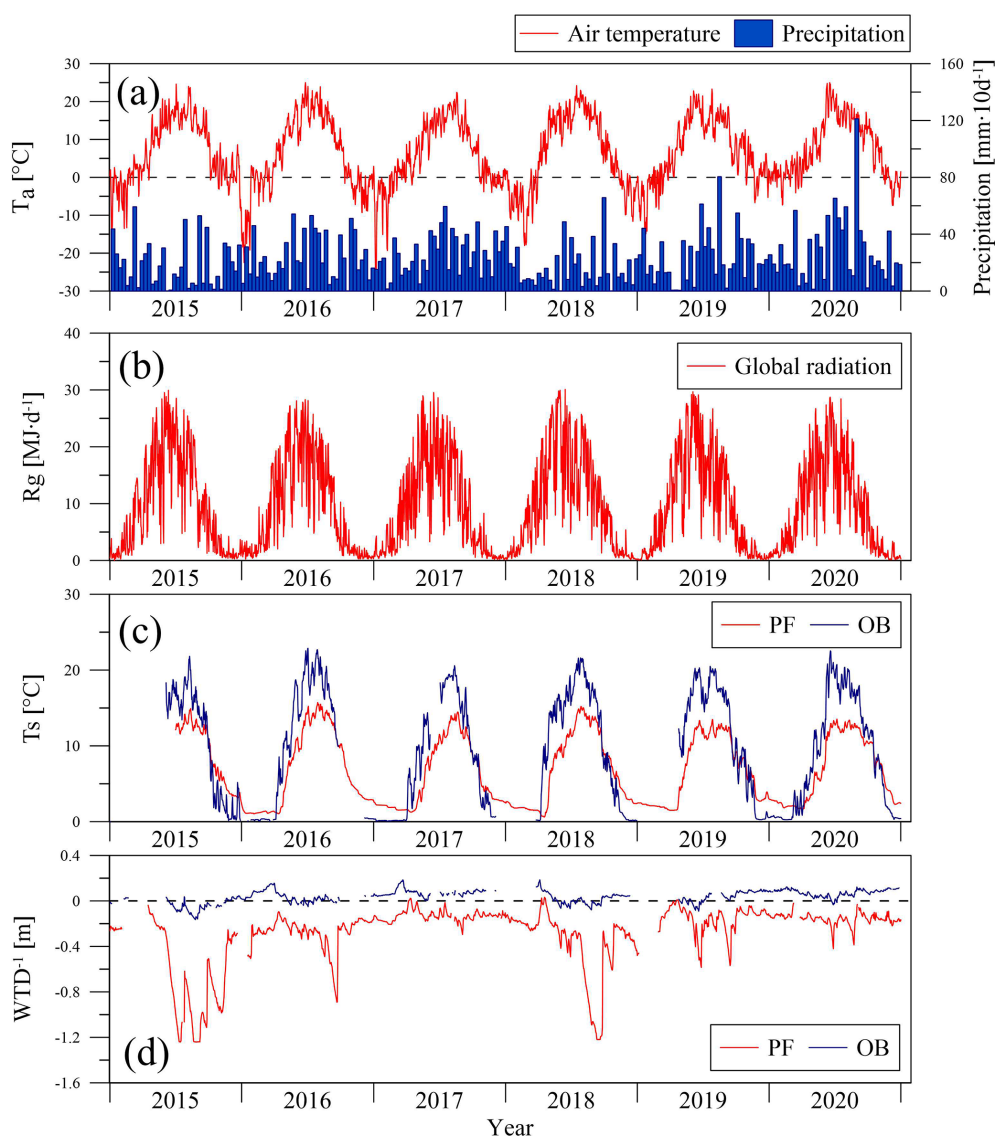
Figure 2. Seasonal variation in mean daily air temperature (T_a) at meteorological station Toropets, 10 d precipitation sums at meteorological station Lesnoy Zapovednik (MS) **(a)**, daily global radiation sums at the paludified forest (PF) **(b)**, mean daily soil temperature at 5 cm depth (T_s) **(c)**, and inverse value of water table depth (WTD^{-1}) at the PF and ombrotrophic bog (OB) sites, correspondingly, in the period 2015–2020.

Table 3. Annual sums of the net ecosystem exchange (NEE), total ecosystem respiration (TER), and gross primary production (GPP), with uncertainty estimates associated with random error in the measured fluxes, u^* threshold estimation, gap-filling and flux partitioning procedures ($\pm$ SD), and GPP/TER ratio at the paludified forest (PF) in the period 2015–2020 and at the ombrotrophic bog (OB) in 2020.

	2015	2016	2017	2018	2019	2020	2020 (OB)
NEE (gC m^{-2})	70 ± 40	145 ± 41	21 ± 48	-30 ± 40	39 ± 42	-62 ± 49	-95 ± 12
TER (gC m^{-2})	1636 ± 66	1652 ± 44	1366 ± 92	1537 ± 43	1631 ± 118	1429 ± 87	410 ± 20
GPP (gC m^{-2})	1566 ± 76	1408 ± 45	1345 ± 89	1566 ± 41	1592 ± 112	1491 ± 102	505 ± 13
GPP/TER	0.96	0.85	0.99	1.02	0.98	1.04	1.23

interannual variability, it is challenging to attribute changes in annual sums of TER and GPP to the environmental conditions in the particular years of the period.

The annual TER and GPP were mainly determined by the growing season sums. Growing season sums (Table 4) of TER and GPP at the PF site (calculated for the long-term climatic growing season 12 April–11 October) made up 84 %–86 % and 90 %–92 %, respectively, in 2015–2019. In 2020, due to the anomalously warm winter 2019/2020 characterized by sparse and thin snow cover, the growing season sums were 76 % of annual TER and 86 % of annual GPP. At the OB site, growing season sums in 2020 were 81 % of annual TER and 92 % of annual GPP. A comparison of the growing season NEE for 2016, 2019, and 2020 at two sites showed that OB site was a CO_2 sink in all selected years, while PF site was a CO_2 source in 2016. Moreover, NEE at the OB site was lower than at the PF site in spite of the lower GPP rates in 2016 and 2019, but in 2020, a lower growing season NEE at the PF site was detected (Table 4). The GPP/TER ratio in the growing season was 0.98–1.12 at the PF site and 1.32–1.40 at the OB site.

Similarly, the lowest winter sums (1 November–31 March) of NEE at the PF site were detected in relatively warm years that are mostly connected with increased GPP. Winter GPP in the warmest winter was higher than in the coldest one (65 %). There was 43 ± 26 gC m^{-2} ($\pm$ SD associated with flux uncertainty) in winter 2017/2018 and 123 ± 17 gC m^{-2} in winter 2019/2020, while TER increased by 28 % (149 ± 27 gC m^{-2} in winter 2017/2018 and 206 ± 16 gC m^{-2} in winter 2019/2020). At the OB site, all the main components of NEE (TER and GPP) were lower than at the PF site in winter. We compared the winter sums of carbon dioxide fluxes at the PF and OB sites for two winter seasons, i.e. winter 2015/2016 with thick and continuous snow cover and the anomalously warm winter of 2019/2020 with thin and sparse snow cover. It was determined that the NEE at the OB site in winter 2019/2020 was slightly higher (40 ± 4 gC m^{-2}) than in winter 2015/2016 (34 ± 5 gC m^{-2}), while the NEE at the PF site in winter 2019/2020 (83 ± 16 gC m^{-2}) was lower than in winter 2015/2016 (115 ± 17 gC m^{-2}). The response of the CO_2 exchange on the anomalously warm weather conditions in winter 2019/2020 at the PF and OB sites was different. At the PF site, the GPP/TER ratio increased from 0.38 in winter 2015/2016 to 0.60 in winter 2019/2020, but at the OB site it slightly decreased from 0.38 to 0.37. At the PF site, GPP and TER were higher in winter 2019/2020 with 42 % and 9 %, respectively, and at the OB site, GPP increased by 8 % and TER by 12 %. Mean daily TER and GPP values at the PF site in winter 2019/2020 were significantly higher than in winter 2015/2016 (M–W U test; $n = 152$, $U = 9355$, $Z = -2.866$, and $p = 0.004$ for TER and $U = 8170$, $Z = -4.413$, and $p < 0.001$ for GPP) and NEE was lower (M–W U test; $n = 152$; $U = 9585$; $Z = 2.566$; $p = 0.010$). At the OB site, a significant difference in the mean daily TER (M–W U test; $n = 152$; $U = 10570$; $Z = -1.281$; $p = 0.200$), GPP (M–

W U test; $n = 152$; $U = 11497$; $Z = 0.07112$; $p = 0.943$), and NEE (M–W U test; $n = 152$; $U = 10499$; $Z = -1.374$; $p = 0.170$) between the winters was not found. Therefore, the warm winter led to the substantial changes in the daily and seasonal CO_2 fluxes at the paludified forest, especially in GPP, and relatively small changes in the daily and seasonal CO_2 fluxes at the bog site.

Lower GPP and TER rates at the OB site compared to the GPP and TER at the PF site were also detected in seasonal variability in all years of measurements (Fig. 3). Maximal daily sums of TER and GPP were observed in summer, where TER reached 19 gC m^{-2} d^{-1} and GPP 18 gC m^{-2} d^{-1} at the PF site, while at the OB site, TER did not exceed 6 gC m^{-2} d^{-1} and GPP 7 gC m^{-2} d^{-1}, respectively. As a result, the seasonal amplitude of NEE at the PF site was more pronounced than at the OB site, and the daily sums of NEE ranged between 7 and -7 gC m^{-2} d^{-1} at the PF site and between 1 and -3 gC m^{-2} d^{-1} at the OB site.

In the 2015–2019 period, the PF site became a sink of atmospheric CO_2 in March (3–7 weeks before the start of the growing season calculated using mean daily air temperature data) and a CO_2 source in late September–mid October. The OB site became a sink after snow-melting in late April (2–4 weeks after the start of the growing season) to the first 10 d of May and a CO_2 source in September. In the warmest year – 2020 – at the PF site, the first days with daily NEE < 0 were observed in mid-February (10 weeks before the start of the growing season), while at the OB site this only occurred at the end of May (5 weeks after the start of the growing season). The shift in the compensation point due to the positive temperature anomaly and lack of snow cover in winter and early spring to the earlier dates at the PF site and later dates at the OB site can be explained by the difference in vegetation composition and its phenology. The primary production of the conifer trees at the PF site in February and March is limited by low air temperatures, and the positive temperature anomaly triggered early CO_2 uptake at the forest site; thus, the GPP at the PF site grew faster than TER. At the OB site, the lack of snow led to the fast heating of the upper peat layer, and consequently, TER increased faster than GPP. In spite of the higher CO_2 uptake at the OB site, the time period when the PF site was a sink of atmospheric CO_2 was longer primarily in spring. Therefore, the weather conditions in spring play an important role in the differences between NEE at a paludified spruce forest and ombrotrophic bog.

3.3 Environmental controls of CO_2 fluxes

The main components of NEE (TER and GPP) varied during the period 2015–2020, following the changes in the different environmental factors. The TER rates at the sites were sensitive to the soil and air temperatures. We used the Q_{10} function (Eq. 1) for parameterizing the dependence of TER on air and soil temperatures at the PF and OB sites (Fig. 4). Only original nighttime data of NEE collected in 12 April–11 Oc-

Table 4. Growing season (calculated for long-term mean growing season 12 April–11 October) sums of net ecosystem exchange (NEE), total ecosystem respiration (TER), gross primary production (GPP), with uncertainty estimates associated with random error in the measured fluxes, u^* threshold estimation, gap-filling and flux partitioning procedures ($\pm$ SD), and GPP/TER ratio at the paludified forest (PF) and at the ombrotrophic bog (OB) in the period 2015–2020.

|	2015	2016		2017	2018	2019		2020	
	PF	PF	OB	PF	PF	PF	OB	PF	OB
NEE (gC m^{-2})	-43 ± 39	28 ± 40	-108 ± 6	-72 ± 38	-135 ± 38	-78 ± 39	-120 ± 8	-142 ± 48	-132 ± 11
TER (gC m^{-2})	1366 ± 58	1317 ± 41	334 ± 10	1135 ± 64	1308 ± 39	1384 ± 110	339 ± 15	1140 ± 83	332 ± 17
GPP (gC m^{-2})	1409 ± 69	1289 ± 42	442 ± 13	1207 ± 66	1443 ± 38	1462 ± 107	458 ± 10	1282 ± 100	464 ± 11
GPP/TER	1.03	0.98	1.32	1.06	1.10	1.06	1.35	1.12	1.40
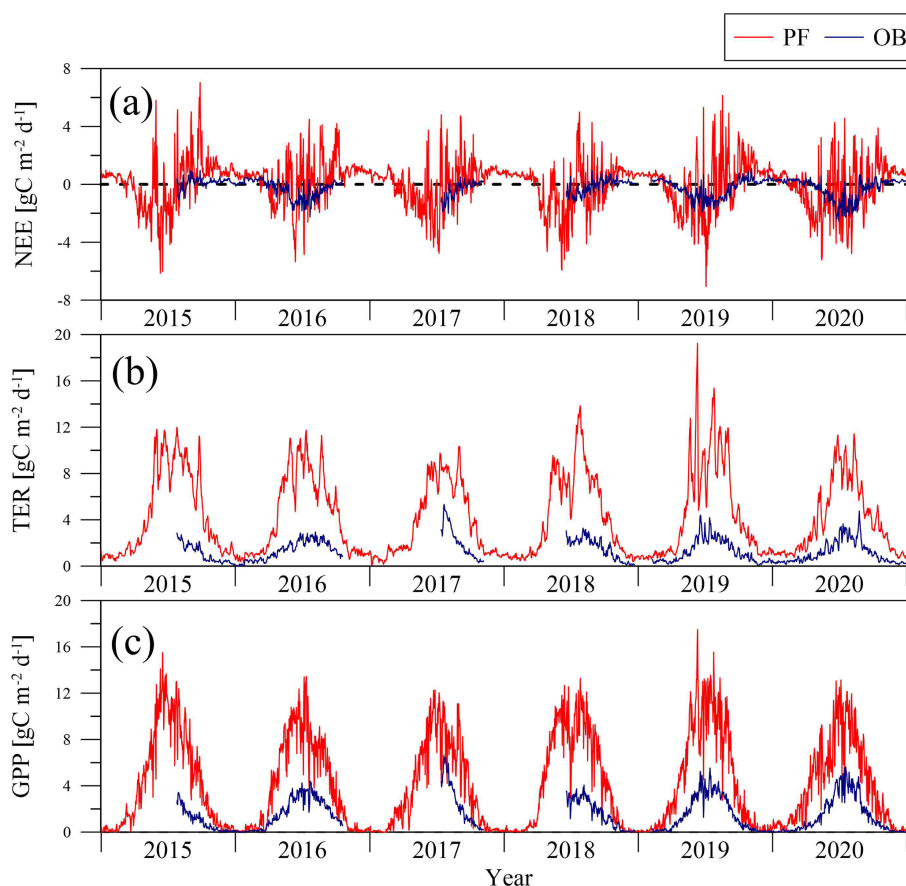
Figure 3. Seasonal variation in the net ecosystem exchange (NEE) **(a)**, total ecosystem respiration (TER) **(b)**, and gross primary production (GPP) **(c)** at the paludified forest (PF) and ombrotrophic bog (OB) sites in the period 2015–2020.

tober period were used for the analysis. The mean nighttime soil temperature at the OB site varied in a wider range than at the PF site, from 3 °C and reaching 25 °C, while at the PF site, it was between 0 and 15 °C. Air temperature variations at night were very similar at the two sites. TER rates in the presented soil and air temperature ranges had a different magnitude at the sites. TER at the PF site reached 16 µmol m^{-2} s^{-1}, while TER at the OB site did not exceed 6 µmol m^{-2} s^{-1}. Moreover, TER at the PF site was on aver-

age higher than at the OB site within the whole presented air and soil temperature ranges.

Maximal Q_{10} values at the PF and OB sites were observed when the soil temperature was used for Q_{10} coefficient calculation, but Q_{10} values were higher at the PF site than at the OB site, if Q_{10} is calculated using soil temperature, and higher at the OB site, if air temperature is used for the calculation (Table 5). Similarly, the maximal R_{10} coefficient at the PF site was obtained using soil temperature and using air temperature at the OB site. Regardless of whether soil or air
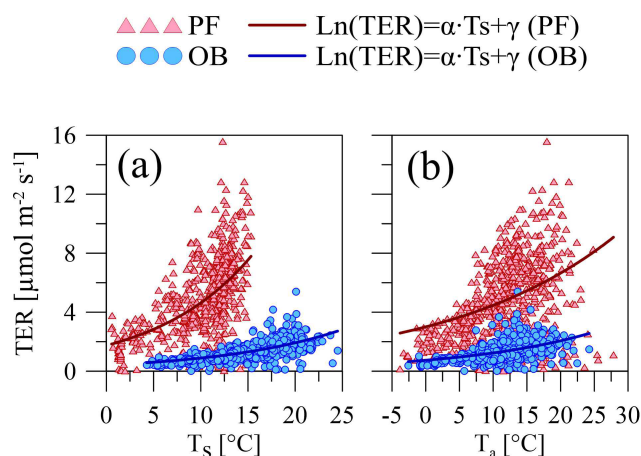
Figure 4. Relationship between the mean nighttime ecosystem respiration (TER) and **(a)** soil (T_s) and **(b)** air temperature (T_a) at the paludified forest (PF) and ombrotrophic bog (OB) sites in the period 12 April–11 October 2015–2020 (approximated using the Q_{10} function; see Eq. 1).
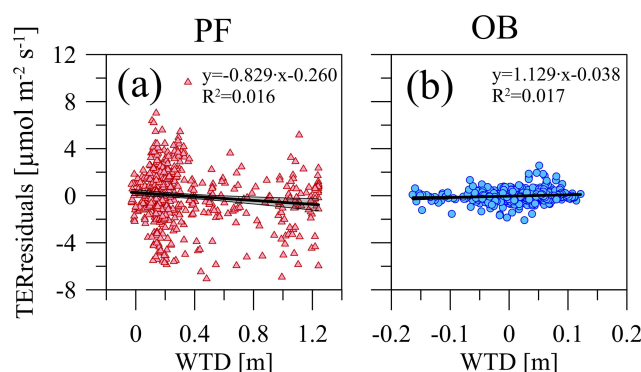
Figure 5. Relationship between the residuals of the Q_{10} model (Fig. 4a and Table 5) calculated using soil temperature and WTD at the **(a)** paludified forest (PF) and **(b)** ombrotrophic bog (OB), with the linear fit and its 95 % confidence interval.

temperature was used, R_{10} at the PF site was higher than at the OB site. The residuals of the Q_{10} models showed a weak dependence on WTD (Fig. 5).

To represent the dependence of GPP at the sites on changes in R_g, we used the hyperbolic light response curve (Eq. 3). Only 30 min of GPP values calculated from the original NEE data were taken for the analysis. To show the seasonal and interannual variations in the curve parameters, we considered the data in different months (April, July, and October) for the anomalously cool and wet growing season of 2017 and the anomalously warm and dry growing season of 2018 (Fig. 6).

April is a beginning of the growing season and characterized by wide range of R_g and a comparatively narrow range of GPP. Unfortunately, the lack of the original NEE data at the OB site in April did not allow us to compare light response curve parameters at the two sites for this month. July

Table 5. Parameters α and γ of Eq. (2) and R^2 ($p < 0.01$) and Q_{10} and R_{10} coefficients calculated using soil (T_s) and air (T_a) temperature at the paludified forest (PF) and ombrotrophic bog sites (OB).

	α	γ	R^2	Q_{10}	R_{10} (μmol m^{-2} s^{-1})
PF (T_s)	0.098	0.556	0.289	2.66	4.65
OB (T_s)	0.077	−0.883	0.431	2.16	0.89
PF (T_a)	0.040	1.100	0.174	1.49	4.48
OB (T_a)	0.051	−0.297	0.261	1.67	1.24

is the middle of the growing season, when R_g and GPP are relatively high. At the end of the growing season (October), both GPP and R_g had a relatively narrow range of variation. It is important to note that GPP at the OB site was lower than at the PF site in all months of the selected years that largely determined the difference in the parameters of the curves between the sites due to the almost equal R_g (the difference in the daily sums between the sites was on average ±3 %).

An analysis of the light response curves (Table 6) showed that, in relatively warm April 2018, the α coefficient (which refers to sensitivity of GPP to R_g) was lower than in relatively cold April 2017, but the β coefficient (which denotes the saturation point of the curve) was higher in April 2018. In July, the α and β coefficients at the PF site were higher in the relatively warm year of 2018 and in the relatively cool year of 2017 at the OB site. In July 2017, α at the PF site was lower than at the OB site, but β was relatively higher. In July 2018, both α and β parameters were higher at the PF site. In October 2017 and 2018, α and β were also higher at the PF site, and the highest values of α at the PF and OB sites were detected in October 2017, while the highest β values were detected in October 2018.

Additionally, we compared the light response curves for March (2018 and 2020), with the last winter months in an anomalously cold and snowy winter 2017/2018 and an anomalously warm winter 2019/2020 with sparse and thin snow cover at the PF site (Fig. 7). Due to the low GPP values, it was quite difficult to establish the dependence between GPP and R_g in March 2018, while the sensitivity of GPP to changes in R_g was pronounced in March 2020, with relatively high GPP in the whole range of R_g, especially at high R_g values. It demonstrated the difference in the response of GPP to interannual changes in environmental conditions at the paludified forest in early spring.

4 Discussion

4.1 Ecosystem CO_2 fluxes

A total of 6 years of paired eddy covariance measurements (2015–2020) at the PF and OB sites showed that ombrotrophic bog in the southern taiga of western Russia was
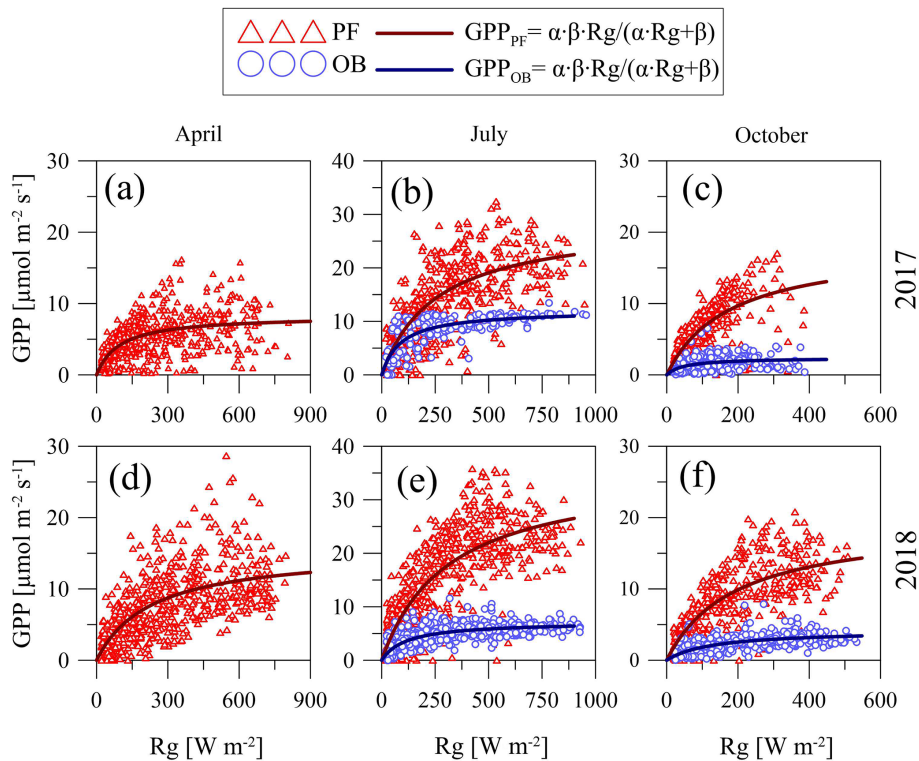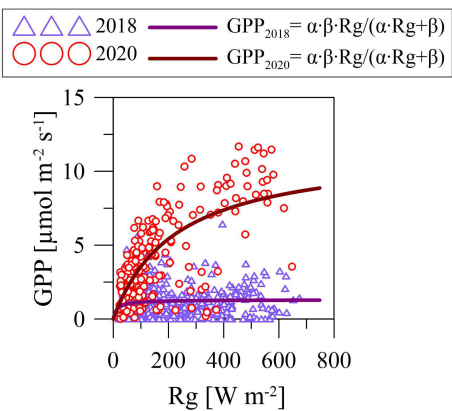
Figure 6. Hyperbolic light response curves (Eq. 3) of gross primary production (GPP) for April **(a, d)**, July **(b, e)**, and October **(c, f)** in 2017 and 2018 at the paludified forest (PF) and ombrotrophic bog (OB) sites.

Table 6. Parameters α and β of the light response curves (Eq. 3) and R^2 ($p < 0.01$) for March, April, July, and October in 2017, 2018, and 2020 at the paludified forest (PF) and the ombrotrophic bog (OB).

	α ($\mu mol\,J^{-1}$)		β ($\mu mol\,m^{-2}\,s^{-1}$)		R^2	
	PF	OB	PF	OB	PF	OB
2017						
April	0.085	–	8.3	–	0.299	–
July	0.112	0.132	28.9	12.1	0.567	0.562
October	0.104	0.048	18.2	2.4	0.542	0.134
2018						
March	0.093	–	1.3	–	0.014	–
April	0.067	–	15.5	–	0.403	–
July	0.114	0.062	35.7	7.2	0.604	0.585
October	0.101	0.032	19.3	4.2	0.610	0.014
2020						
March	0.05	–	11.5	–	0.485	–

Figure 7. Hyperbolic light response curves (Eq. 3) of gross primary production (GPP) for March 2018 and 2020 at the paludified forest (PF).

a stronger CO_2 sink in the growing season than the adjacent paludified spruce forest, except for the warmest year of the period. However, the paludified spruce forest had a greater annual growing season and daily TER and GPP than the adjacent bog. Therefore, under the described environmental conditions, the difference in the annual and growing season

CO_2 uptake of the ecosystems was mostly dependent on a specific GPP/TER ratio rather than on a difference in GPP. The growing season GPP/TER ratio was 0.98–1.12 at the PF site and 1.32–1.40 at the OB site, and the annual value changed between 0.85 and 1.04 at the PF site and was 1.23 at the OB site in 2020. The annual and growing season values of the GPP/TER ratio at the PF site corresponded to the values obtained in an old spruce forest on mineral soils lo-

cated 2 km to the south of the PF site (0.98; Mamkin et al., 2019) and for black spruce (*Picea mariana*) stands on peaty soils, reported by Dunn et al. (2007) in Manitoba (Canada; annual 0.89–1.09), Ueyama et al. (2014; annual 0.85–1.41; growing season 0.90–1.61), and Euskirchen et al. (2014; annual was about 1.04 and the growing season 1.14-1.47, with the annual GPP/TER ratio for the adjacent bog site of about 1.08 and 1.30–1.42 in the growing season) for permafrost in Alaska (USA). The GPP/TER ratio for the OB site is also in agreement with the growing season values reported by Sulman et al. (2010) for bogs in Wisconsin (USA) (1.03) and Ontario (Canada) (1.30), but it was lower than the GPP/TER ratio for bog in western Siberia (2.29) obtained by Aleksey-chik et al. (2017) in May–August.

In spite of numerous experiments focused on CO_2 fluxes at boreal and temperate peatlands (e.g. Martikainen et al., 1995; Lafleur et al., 2001; Aurela et al., 2002; Lindroth et al., 2007; Petrescu et al., 2015), it is a small number of studies that are based on simultaneous flux measurements at spruce forests and bogs located in the same landscape and undergoing similar weather conditions. The estimates of NEE at the OB and PF sites (Tables 3 and 4) are similar to the annual NEE obtained by Euskirchen et al. (2014) for permafrost in Alaska (USA) during the 3 years of measurements (between -76 and $72\,\mathrm{gC\,m^{-2}\,yr^{-1}}$ at a black spruce forest and between -81 and $23\,\mathrm{gC\,m^{-2}\,yr^{-1}}$ at the bog) and TER and GPP sums at the OB site (465–519 and 496–548 $\mathrm{gC\,m^{-2}\,yr^{-1}}$ for TER and GPP, respectively), while the annual TER and GPP at a black spruce forest was significantly lower than at the PF site (491–633 and 544–588 $\mathrm{gC\,m^{-2}\,yr^{-1}}$ for TER and GPP, respectively). The similar annual and growing season NEE and larger TER and GPP sums at the PF site in comparison with data from other black spruce stands was also detected. For example, Ueyama et al. (2014) reported that the growing season (April–September) sums of TER and GPP at the black spruce stand on permafrost in Alaska varied between 403–759 and 491–799 $\mathrm{gC\,m^{-2}}$, respectively, and the corresponding NEE values changed from -93 to $15\,\mathrm{gC\,m^{-2}}$ during the 9 years of measurements. So, the black spruce stand was primarily a sink of atmospheric CO_2. Dunn et al. (2007) also examined CO_2 fluxes in an old black spruce forest in Manitoba (Canada) during the 9 years of measurements and found that annual NEE was -8 and $54\,\mathrm{gC\,m^{-2}}$, with annual TER 611–826 $\mathrm{gC\,m^{-2}\,yr^{-1}}$ and GPP 610–782 $\mathrm{gC\,m^{-2}\,yr^{-1}}$. NEE and TER and GPP at the PF site were also similar to the estimates for the adjacent old spruce forest on mineral soils, namely NEE from April to mid-October 2016 was $24\,\mathrm{gC\,m^{-2}}$, with corresponding TER $= 1373\,\mathrm{gC\,m^{-2}}$ and GPP $= 1349\,\mathrm{gC\,m^{-2}}$ (Mamkin et al., 2019). The relatively warm and wet weather conditions with a long growing season and nutrient availability in the southern taiga of Valdai Hills provide favourable conditions for photosynthesis and ecosystem respiration of the boreal forests (Karpov, 1983). But its annual CO_2 uptake under the environmental

conditions close to the long-term means is similar to the estimates from the other boreal forests located in colder climate and is, moreover, lower than the annual uptake at the bogs of the same landscape.

Larger CO_2 uptake at the Siberian spruce (*Picea obovata* Ledeb.) forest on peaty soils than at mesotrophic peatland located in 40 km from the forest in the northern Ural (Komi Republic, Russia) in April–August was measured by Zagirova et al. (2019), where NEE at the forest was -327 and $-140\,\mathrm{gC\,m^{-2}}$ at the mesotrophic peatland. NEE and TER and GPP sums for the OB site also corresponded to the estimates from other studies. For example, the NEE of the bog in western Siberia in the period May–August, as estimated by Alekseychik et al. (2017), was $-20\,\mathrm{gC\,m^{-2}}$ with corresponding TER and GPP values of 157 and 359 $\mathrm{gC\,m^{-2}}$, respectively. The Annual NEE at the bog in southern Sweden, reported by Lund et al. (2007), was $-21.5\,\mathrm{gC\,m^{-2}}$.

Interannual variability and the long-term trends in the environmental conditions could substantially influence annual NEE at the southern taiga peatlands. The NEE estimated at the PF site in 2015–2020 (Table 3) was lower than the NEE reported by Kurbatova et al. (2008) and was measured at the same site in 1999–2004 (100–600 $\mathrm{gC\,m^{-2}\,yr^{-1}}$). The difference could be explained by a positive air temperature trend in the last 20 years that enhanced GPP at the site and increased in annual precipitation, which therefore provided a decrease in WTD and consequently inhibited TER. The increase in the CO_2 uptake at the PF site due to the lowering of the WTD is in agreement with model experiments carried out by Kurbatova et al. (2008).

Interannual variation in the growing season NEE at the PF and OB sites and interannual variation in annual NEE in 2015–2020 is explained by changes in both TER and GPP rates, and the maximal GPP values were observed in the years with increased R_g. A previous study at the PF and OB sites (Kurbatova et al., 2013) demonstrated that TER plays a key role in the NEE of the sites, especially in the relatively warm years. It is correspondent with the work of Dunn et al. (2007), Ueyama et al. (2014) and Euskirchen et al. (2014), who showed that interannual changes in annual NEE of the black spruce stands in Alaska (USA) and Manitoba (Canada) were primarily dependent on TER variability than on changes in GPP. A strong dependence of NEE on TER was also obtained for a fen in Alberta (Canada) by Cai et al. (2010).

It is considered that relatively warm and dry weather conditions usually increase TER rates at the peatlands due to the enhanced soil and air temperature, and WTD and can shift a peatland from a CO_2 sink to a CO_2 source (Moore, 2002; Drösler et al., 2008; Minkinnen et al., 2018). Thus, the drought events can be the major environmental factor causing interannual variations in NEE at the peatlands and controlling the TER rates (Welp et al., 2007; Lund et al., 2012). It is consistent with the chamber measurements at the OB site performed in the previous years and includes an ex-

treme drought 2010 in western Russia (Ivanov et al., 2017; Kurbatova et al., 2013). It is important to note that respiration rates measured by chambers and reported by Kurbatova et al. (2013) reached the maximum values and were more sensitive to temperature variations under the weather conditions close to the long-term means in summer. Under the low WTD in the snow-melting period of spring and in the extreme drought of 2010 (with WTD > 35 cm), respiration rates were lower and less sensitive to the temperature variations. In the period 2015–2020, there were not such extreme droughts, and relatively low WTD variation was observed at the OB site. At the PF site, a substantial increase in the WTD was detected in the growing seasons with the negative precipitation anomaly. An increased annual and growing season, TER, was detected in the years with a high WTD. But 30 min and mean nighttime TER on WTD were dependent on WTD variations. Therefore, the air and soil temperatures were the main predictors of seasonal variations in TER at the sites in the selected years.

The weak dependence of TER and NEE to WTD at the peatlands was reported in many studies (e.g. Lafleur et al., 2001, 2005; Parmentier et al., 2009; Sulman et al., 2009; Alekseychik et al., 2017). For example, Parmentier et al. (2009) hypothesized that increasing WTD will affect TER on peatland if WTD changes are accompanied by changes in soil water content. Lafleur et al. (2005) suggested that dependence of TER on WTD is a result of complex interactions between WTD, vertical profiles of peat water content in the unsaturated zone above the water table, and vertical profiles of peat decomposability, and they supposed that TER at wetter peatlands would be more sensitive to changes in WTD. Sulman et al. (2009) detected that a lower water level increases both TER and GPP and leads to a small dependence of NEE on the peatland to changes in WTD. It is feasible that small changes in WTD and uniform distribution of precipitation during the study period preserved the peat layer properties at the PF and OB sites, and the strong dependence of TER and NEE on WTD would be detectable if droughts were more frequent in the region.

The sensitivity parameters of TER (Q_{10}) to soil and air temperatures (Tables 5 and 6) corresponded to the values obtained in other studies (Lafleur et al., 2005; Humphreys et al., 2006; Lindroth et al., 2007; Lund et al., 2007; Ueyama et al., 2014). For example, Humphreys et al. (2006) obtained mid-summer Q_{10} values calculated using air temperature for a bog and different fens in Canada between 1.3–2.0, and R_{10} was 0.9–3.2 μmol m^{-2} s^{-1}. Lund et al. (2007) reported that Q_{10} at the temperate bog in Sweden was 1.81 when air temperature was used for the calculation, and 2.83 was obtained when using the soil temperature at 5 cm depth. Also, slightly different Q_{10} values were obtained, depending on microtopography of the bog. The corresponding Q_{10} values were 2.32 and 2.54 for hummocks and for hollows. Lafleur et al. (2005) estimated Q_{10} values of 2.24 when air temperature at 50 cm height was used, with 2.57 at the hummock

and 3.91 at the hollow, at the bog in Ontario (Canada). Q_{10} values at the black spruce stand in Alaska (USA) in the growing season were reported by Ueyama et al. (2014) and calculated using air temperature ranged between 1.5–2.5. However, Q_{10} values calculated for the PF site were lower than for adjacent spruce forest on mineral soils in the growing season 2016, with 2.49 and 5.77 calculated using air and soil temperature, respectively, and reported by Mamkin et al. (2019). The corresponded R_{10} values were 5.43 and 5.77, respectively. The lower sensitivity of TER at the PF and OB sites in comparison with the adjacent forest on mineral soils could be connected with both decreased heterotrophic and autotrophic respiration due to the paludification, which inhibits decomposition processes in the upper soil layers and limits the productivity of the ecosystems.

4.2 Uncertainty in the seasonal and annual ecosystem CO_2 fluxes

Uncertainty associated with random error in the measured fluxes and data processing was about 2 %–8 % of the annual and growing season TER and GPP at the sites and exceeded annual and growing season NEE in several years at the PF site. Considering the uncertainty in the CO_2 flux estimates it is difficult to identify the current status of PF as atmospheric CO_2 source or sink straightforward. It is likely that annual NEE at the PF site is close to 0 but in most of the growing seasons of the period it was a sink. Unlike PF site, OB site had lower NEE uncertainty than the growing season and annual (in 2020) net CO_2 uptake rates, hence OB site is functioning as a CO_2 sink for the atmosphere. Although an increase in the CO_2 sequestration by PF site and GPP/TER ratio was observed in the warmest 2020 year and decreased TER and GPP values in the coldest 2017 year it is challenging to attribute interannual changes in CO_2 fluxes with the environmental conditions in other years due to the range of uncertainty similar to the interannual flux variability.

4.3 Implications of climate change in the region for peatlands

The observed warming trend in the boreal ecozone led to the increase in both TER and GPP (Aurela et al., 2004; Minkkinen et al., 2018; IPCC, 2019). But the net effect on NEE (shifting the ecosystem status to a CO_2 source or a CO_2 sink for the atmosphere) can vary across the ecosystems, depending on local environmental conditions, hydrology, and vegetation type. The 6 years of eddy covariance measurements at the PF and OB sites showed that a positive temperature anomaly can increase the proportion of the winter fluxes to the annual sums. At the PF site, a positive anomaly in the winter months mainly increases the production and decomposition processes (mainly GPP), while at the OB site, changes in TER and GPP are not significant. The winter NEE in boreal peatlands is usually dependent on the TER

rates (Fahnestock et al., 1999; Koehler et al., 2011; Lohila et al., 2011). The growth of winter air and soil temperature can potentially increase the CO$_2$ release. Several studies have shown that winter emission in boreal peatlands can offset the summer CO$_2$ uptake (Alm et al., 1999; Lafleur et al., 2001; D'Acunha et al., 2019).

Previous studies carried out at the same sites, using eddy covariance and chamber measurements and modelling experiments (Milyukova et al., 2002; Kurbatova et al., 2008, 2013), suggested that climate warming can increase the TER and, consequently, NEE of the bogs and paludified forests in the region. In this study, we estimated that the interannual variability in GPP driven by a temperature anomaly can substantially influence the annual and seasonal NEE of the selected ecosystems, and the positive temperature anomaly leads to the increase in the CO$_2$ uptake of the paludified forest. It is in keeping with Dunn et al. (2007), who showed that a black spruce forest on peaty soils in Manitoba (Canada) switched from a CO$_2$ source to a CO$_2$ sink in the several years following a positive temperature trend. The different response of NEE to a positive temperature anomaly in previous studies and in the present research is likely connected with difference in the moisture regime at the PF and OB sites between 1999–2011 and 2015–2020. So, under hot and dry conditions, the ecosystems were a CO$_2$ source for the atmosphere, which is in agreement with several studies of similar ecosystems (Lund et al., 2007; Cai et al., 2010). It is likely that the increase in precipitation during the last few decades, which was uniformly distributed over a growing season period, provided a low WTD and created a favourable conditions for growing in GPP and the increase in the CO$_2$ uptake at the sites.

The influence of the present warming trend on NEE of the peatlands is also dependent on the season in which the substantial changes in air temperature and precipitation are observed. The shifting of the growing season start and the snow-melting period can additionally impact the annual NEE. For example, late snow-melting and the late start of the growing season, followed by a hot and dry summer in Alaska (USA), switched a black spruce permafrost forest and its adjacent bog from being a CO$_2$ sink (under temperature and precipitation close to the long-term means) to a CO$_2$ source for the atmosphere (Euskirchen et al., 2014). Conversely, the early start of the growing season and snow-melting can lead to increasing annual CO$_2$ uptake, and therefore, the environmental conditions in spring can determine the annual CO$_2$ balance of the forest and bog ecosystems that was reported in many experimental studies (Lafleur et al., 2001; Aurela et al., 2004; Syed et al., 2006; Black et al., 2000; Hommeltenberg et al., 2014). However, the research provided by Goulden et al. (1998) showed that a positive air temperature trend in spring can lead to a substantial carbon loss in an old black spruce forest in Manitoba (Canada). An important factor of the spring NEE can be a thaw water supply. For example, Hu et al. (2010) reported that early sea-

sonal warming with a lack of thaw water in spring decreased the CO$_2$ uptake of a subalpine pine–aspen forest in Colorado Rocky Mountains (USA).

The response of CO$_2$ fluxes at the PF and OB sites to the positive temperature anomaly in spring was different. CO$_2$ uptake at the paludified spruce forest began before the snow-melting, and the anomalously warm conditions in late winter and early spring provided a substantial increase in GPP, while the CO$_2$ uptake at the bog was observed after the start of the growing season. Thus, we expect that the increase in the frequency of thawing weather periods in winter that was predicted in western Russia (Roshydromet, 2014; IPCC, 2014) and in early spring can increase the CO$_2$ uptake of the paludified forest, with less significant changes in NEE at the bog. Unlike warm springs, a warm autumn can increase TER more than GPP and, consequently, reduce an annual CO$_2$ sequestration (Piao et al., 2008; Ueyama et al., 2014).

According to the meteorological observations during the last 30 years, the mean annual air temperature and annual precipitation on Valdai Hills show a positive trends in the last few decades, which is mostly connected with the increase in winter temperature and precipitation. However, the thickness of snowpack and the period with snow cover is decreasing. Moreover, the growing season became longer, primarily due to the shifting of the start of the growing season to earlier dates in spring, with no significant shift in the end of the growing season in autumn. According to the current climate changes, an increase in the CO$_2$ sequestration at peatlands due to the enhanced GPP rates, especially at forest ecosystems, in early spring in the western part of Valdai Hills is expected. However, the latest climate predictions (IPCC, 2021) for the region showed that future warming in the next few decades will be combined with precipitation increasing in winter and decreasing in summer. Thus, in spite of the positive trend in annual precipitation, a raising frequency of heatwaves and droughts in summer is also presumable. While warming and moistening in winter could increase the GPP more than TER, especially at paludified forests, the extreme hot and dry conditions are able to increase heterotrophic respiration significantly and switch peatlands from a CO$_2$ sink to a consistent CO$_2$ source for the atmosphere and alter the NPP (net primary production) of the ecosystems. For example, the SPRUCE experiment in Minnesota (USA) showed significant carbon loss rates at black spruce stands on the bog (higher than its historical accumulation rates) under the warming treatment, which was connected with increased heterotrophic respiration and decreased *Sphagnum* NPP and aboveground NPP of trees (Walker et al., 2017; Hanson et al., 2020).

Noting that the PF site is characterized by high interannual variability in NEE, which is close to 0, and a relatively high daily, growing season, and annual TER and GPP, as well as a high sensitivity of TER and GPP to the changes in environmental factors, the observed warming trend can affect the status of the paludified forests in the southern taiga as a source

or sink of atmospheric CO$_2$ more than bogs located in the same landscape. Therefore, we can expect an increasing role of the moistening conditions under future climate change for the ecosystem status as a source or sink of atmospheric CO$_2$ in the southern taiga of western Russia.

5 Conclusions

The 6 years of paired eddy covariance CO$_2$ flux measurements at a paludified spruce forest and an adjacent ombrotrophic bog in the southern taiga of western Russia during 2015–2020 showed that the PF site had higher daily, growing season, and annual TER and GPP rates, and its sensitivity to the environmental variables was higher than at the OB site. The OB site was a sink of atmospheric CO$_2$ (NEE < 0) in the growing seasons, with higher GPP/TER ratios, while PF was a CO$_2$ source or sink, with the annual and growing season NEE close to zero. Considering the high variability in TER and GPP rates, PF can be a stronger CO$_2$ sink than the OB site in particular years (e.g. in 2020). A positive temperature anomaly in winter 2019/2020 led to the increased daily GPP and TER values and GPP/TER ratio at the PF site in non-growing season, especially in early spring. At the OB site, the changes in TER, GPP, and NEE between the relatively cold and warm winters were not significant. The increased daily GPP/TER ratio in the warmest and the wettest year of the period (2020) at the PF site was detected. Therefore, the positive temperature anomaly in late winter and early spring can potentially increase the CO$_2$ uptake of the southern taiga paludified spruce forests more than for the bogs in the same landscapes. However, if the drought events associated with the expected climate change will be more frequent in the region, then the increase in TER rates can overlap the effect of increasing GPP rates and switch the paludified forest to a consistent CO$_2$ source for the atmosphere. We also expect the increasing role of the moistening conditions to regulate the future status of the southern taiga peatlands as a carbon dioxide source or sink under the warming trend.

Author contributions. VM designed the study, performed the data analysis and field measurements at the PF site, and wrote the majority of the text. VA designed and performed the field measurements at the OB site. DI performed the field measurements and data processing. AV designed the study and field measurements at the PF site. JK designed the study and wrote the text.

References

Alekseychik, P., Mammarella, I., Karpov, D., Dengel, S., Terentieva, I., Sabrekov, A., Glagolev, M., and Lapshina, E.: Net ecosystem exchange and energy fluxes measured with the eddy covariance technique in a western Siberian bog, Atmos. Chem. Phys., 17, 9333–9345, https://doi.org/10.5194/acp-17-9333-2017, 2017.

Alexandrov, G. A., Brovkin, V. A., Kleinen, T., and Yu, Z.: The capacity of northern peatlands for long-term carbon sequestration, Biogeosciences, 17, 47–54, https://doi.org/10.5194/bg-17-47-2020, 2020.

Alm, J., Schulman, L., Walden, J., Nykänen, H., Martikainen, P. J., and Silvola, J.: Carbon balance of a boreal bog during a year with an exceptionally dry summer, Ecology, 80, 161–174, https://doi.org/10.1890/0012-9658(1999)080[0161:CBOABB]2.0.CO;2, 1999.

Aurela, M., Laurila, T., and Tuovinen, J. P.: Annual CO$_2$ balance of a subarctic fen in northern Europe: Importance of the wintertime efflux, J. Geophys. Res.-Atmos., 107, ACH 17-1–ACH 17-12, https://doi.org/10.1029/2002JD002055, 2002.

Aurela, M., Laurila, T., and Tuovinen, J. P.: The timing of snow melt controls the annual CO$_2$ balance in a subarctic fen, Geophys. Res. Lett., 31, L16119, https://doi.org/10.1029/2004GL020315, 2004.

Beaulne, J., Garneau, M., Magnan, G., and Boucher, É.: Peat deposits store more carbon than trees in forested peatlands of the boreal biome, Sci. Rep.-UK, 11, 1–11, https://doi.org/10.1038/s41598-021-82004-x, 2021.

Black, T. A., Chen, W. J., Barr, A. G., Arain, M. A., Chen, Z., Nesic, Z., Hogg, E. H., Neumann, H. H., and Yang, P. C.: Increased carbon sequestration by a boreal deciduous forest in years with a warm spring, Geophys. Res. Lett., 27, 1271–1274, https://doi.org/10.1029/1999GL011234, 2000.

Buitenwerf, R., Rose, L., and Higgins, S. I.: Three decades of multidimensional change in global leaf phenology, Nat. Clim. Change, 5, 364–368, https://doi.org/10.1038/nclimate2533, 2015.

Cai, T., Flanagan, L. B., and Syed, K. H.: Warmer and drier conditions stimulate respiration more than photosynthesis in a boreal peatland ecosystem: analysis of automatic chambers and eddy covariance measurements, Plant Cell Environ., 33, 394–407, https://doi.org/10.1111/j.1365-3040.2009.02089.x, 2010.

D'Acunha, B., Morillas, L., Black, T. A., Christen, A., and Johnson, M. S.: Net ecosystem carbon balance of a peat bog undergoing restoration: integrating CO$_2$ and CH$_4$ fluxes from eddy covariance and aquatic evasion with DOC drainage fluxes, J. Geophys. Res.-Biogeo., 124, 884–901, https://doi.org/10.1029/2019JG005123, 2019.

Desherevskaya, O., Kurbatova, J., and Olchev, A.: Climatic conditions of the south part of Valday Hills, Russia, and their projected changes during the 21st century, Open Geogr. J., 3, 73–79, https://doi.org/10.2174/1874923201003010073, 2010.

Donat, M. G., Alexander, L. V., Yang, H., Durre, I., Vose, R., Dunn, R. J. H., Willett, K. M., Aguilar, E., Brunet, M., Caesar, J., Hewitson, B., Jack, C., Klein Tank, A. M. G., Kruger, A. C., Marengo, J., Peterson, T. C., Renom, M., Oria Rojas, C., Rusticucci, M., Salinger, J., Elrayah, A. S., Sekele, S. S., Srivastava, A. K., Trewin, B., Villarroel, C., Vincent, L. A., Zhai, P., Zhang, X., and Kitching S.: Updated analyses of temperature and precipitation extreme indices since the beginning of the twentieth century: The HadEX2 dataset, J. Geophys. Res.-Atmos., 118, 2098–2118, https://doi.org/10.1002/jgrd.50150, 2013.

Drösler, M., Freibauer, A., Christensen, T. R., and Friborg, T.: Observations and status of peatland greenhouse gas emissions in Europe, in: The Continental-Scale Greenhouse Gas Balance of Europe, Ecological Studies, edited by: Dolman, A. J., Valentini, R., and Freibauer, A., Springer, New York, USA, 243–261, https://doi.org/10.1007/978-0-387-76570-9_12, 2008.

Dunn, A. L., Barford, C. C., Wofsy, S. C., Goulden, M. L., and Daube, B. C.: A long-term record of carbon exchange in a boreal black spruce forest: Means, responses to interannual variability, and decadal trends, Global Change Biol., 13, 577–590, https://doi.org/10.1111/j.1365-2486.2006.01221.x, 2007.

Euskirchen, E. S., Edgar, C. W., Turetsky, M. R., Waldrop, M. P., and Harden, J. W.: Differential response of carbon fluxes to climate in three peatland ecosystems that vary in the presence and stability of permafrost, J. Geophys. Res.-Biogeo., 119, 1576–1595, https://doi.org/10.1002/2014JG002683, 2014.

Fahnestock, J. T., Jones, M. H., and Welker, J. M.: Wintertime CO$_2$ efflux from arctic soils: implications for annual carbon budgets, Global Biogeochem. Cy., 13, 775–779, https://doi.org/10.1029/1999GB900006, 1999.

Friedlingstein, P., Jones, M. W., O'Sullivan, M., Andrew, R. M., Hauck, J., Peters, G. P., Peters, W., Pongratz, J., Sitch, S., Le Quéré, C., Bakker, D. C. E., Canadell, J. G., Ciais, P., Jackson, R. B., Anthoni, P., Barbero, L., Bastos, A., Bastrikov, V., Becker, M., Bopp, L., Buitenhuis, E., Chandra, N., Chevallier, F., Chini, L. P., Currie, K. I., Feely, R. A., Gehlen, M., Gilfillan, D., Gkritzalis, T., Goll, D. S., Gruber, N., Gutekunst, S., Harris, I., Haverd, V., Houghton, R. A., Hurtt, G., Ilyina, T., Jain, A. K., Joetzjer, E., Kaplan, J. O., Kato, E., Klein Goldewijk, K., Korsbakken, J. I., Landschützer, P., Lauvset, S. K., Lefèvre, N., Lenton, A., Lienert, S., Lombardozzi, D., Marland, G., McGuire, P. C., Melton, J. R., Metzl, N., Munro, D. R., Nabel, J. E. M. S., Nakaoka, S.-I., Neill, C., Omar, A. M., Ono, T., Peregon, A., Pierrot, D., Poulter, B., Rehder, G., Resplandy, L., Robertson, E., Rödenbeck, C., Séférian, R., Schwinger, J., Smith, N., Tans, P. P., Tian, H., Tilbrook, B., Tubiello, F. N., van der Werf, G. R., Wiltshire, A. J., and Zaehle, S.: Global Carbon Budget 2019, Earth Syst. Sci. Data, 11, 1783–1838, https://doi.org/10.5194/essd-11-1783-2019, 2019.

Gill, A. L., Giasson, M. A., Yu, R., and Finzi, A. C.: Deep peat warming increases surface methane and carbon dioxide emissions in a black spruce-dominated ombrotrophic bog, Global Change Biol., 23, 5398–5411, https://doi.org/10.1111/gcb.13806, 2017.

Gorham, E.: Northern peatlands: role in the carbon cycle and probable responses to climatic warming, Ecol. Appl., 1, 182–195, https://doi.org/10.2307/1941811, 1991.

Goulden, M. L., Wofsy, S. C., Harden, J. W., Trumbore, S. E., Crill, P. M., Gower, S. T., Fries, T., Daube, B. C., Fand, S.-M., Sutton, J., Bazzaz, A., and Munger, J. W.: Sensitivity of boreal forest carbon balance to soil thaw, Science, 279, 214–217, https://doi.org/10.1126/science.279.5348.214, 1998.

Greco, S. and Baldocchi, D. D.: Seasonal variations of CO$_2$ and water vapour exchange rates over a temperate deciduous forest, Global Change Biol., 2, 183–197, https://doi.org/10.1111/j.1365-2486.1996.tb00071.x, 1996.

Hanson, P. J., Griffiths, N. A., Iversen, C. M., Norby, R. J., Sebestyen, S. D., Phillips, J. R., Chanton, J. P., Kolka, R. K., Malhotra, A., Oleheiser, K. C., Warren, J. M., Shi, X., Yang, X., Mao, J., and Ricciuto, D. M.: Rapid net carbon loss from a whole-ecosystem warmed Peatland, AGU Adv., 1, e2020AV000163, https://doi.org/10.1029/2020AV000163, 2020.

Helbig, M., Chasmer, L. E., Desai, A. R., Kljun, N., Quinton, W. L., and Sonnentag, O.: Direct and indirect climate change effects on carbon dioxide fluxes in a thawing boreal forest-wetland landscape, Global Change Biol., 23, 3231–3248, https://doi.org/10.1111/gcb.13638, 2017.

Helbig, M., Humphreys, E. R., and Todd, A.: Contrasting temperature sensitivity of CO$_2$ exchange in peatlands of the Hudson Bay Lowlands, Canada, J. Geophys. Res.-Biogeo., 124, 2126–2143, 2019.

Helbig, M., Waddington, J. M., Alekseychik, P., Amiro, B., Aurela, M., Barr, A. G., Black, T. A., Carey, S. K., Chen, J., Chi, J., Desai, A. R., Dunn, A., Euskirchen, E. S., Flanagan, L. B., Friborg, T., Garneau, M., Grelle, A., Harder, S., Heliasz, M., Humphreys, E. R., Ikawa, H., Isabelle, P.-E., Iwata, H., Jassal, R., Korkiakoski, M., Kurbatova, J., Kutzbach, L., Lapshina, E., Lindroth,

A., Ottosson Löfvenius, M., Lohila, A., Mammarella, I., Marsh, P., Moore, P. A., Maximov, T., Nadeau, D. F., Nicholls, E. M., Nilsson, M. B., Ohta, T., Peich, M., Petrone, R. M., Prokushkin, A., Quinton, W. L., Roulet, N., Runkle, B. R. K., Sonnentag, O., Strachan, I. B., Taillardat, P., Tuittila, E.-S., Tuovinen, J.-K., Turner, J., Ueyama, M., Varlagin, A., Vesala, T., Wilmking, M., Zyrianov, V., and Schulze, C.: The biophysical climate mitigation potential of boreal peatlands during the growing season, Environ. Res. Lett., 15, 104004, https://doi.org/10.1088/1748-9326/abab34, 2020.

Holl, D., Pfeiffer, E.-M., and Kutzbach, L.: Comparison of eddy covariance CO_2 and CH_4 fluxes from mined and recently rewetted sections in a northwestern German cutover bog, Biogeosciences, 17, 2853–2874, https://doi.org/10.5194/bg-17-2853-2020, 2020.

Hommeltenberg, J., Schmid, H. P., Drösler, M., and Werle, P.: Can a bog drained for forestry be a stronger carbon sink than a natural bog forest?, Biogeosciences, 11, 3477–3493, https://doi.org/10.5194/bg-11-3477-2014, 2014.

Hu, J. I. A., Moore, D. J., Burns, S. P., and Monson, R. K.: Longer growing seasons lead to less carbon sequestration by a subalpine forest, Global Change Biol., 16, 771–783, https://doi.org/10.1111/j.1365-2486.2009.01967.x, 2010.

Humphreys, E. R., Lafleur, P. M., Flanagan, L. B., Hedstrom, N., Syed, K. H., Glenn, A. J., and Granger, R.: Summer carbon dioxide and water vapor fluxes across a range of northern peatlands, J. Geophys. Res.-Biogeo., 111, G04011, https://doi.org/10.1029/2005JG000111, 2006.

IPCC: Climate Change 2014: Synthesis Report, in: Contribution of Working Groups I, II and III to the Fifth Assessment Report of the Intergovernmental Panel on Climate Change, edited by: Core Writing Team, Pachauri, R. K., and Meyer, L. A., IPCC, Geneva, Switzerland, 151 pp., https://www.ipcc.ch/site/assets/uploads/2018/05/SYR_AR5_FINAL_full_wcover.pdf (last access: 11 March 2022), 2014.

IPCC: Climate Change and Land: an IPCC special report on climate change, desertification, land degradation, sustainable land management, food security, and greenhouse gas fluxes in terrestrial ecosystems, edited by: Shukla, P. R., Skea, J., Calvo Buendia, E., Masson-Delmotte, V., Pörtner, H.-O., Roberts, D. C., Zhai, P., Slade, R., Connors, S., van Diemen, R., Ferrat, M., Haughey, E., Luz, S., Neogi, S., Pathak, M., Petzold, J., Portugal Pereira, J., Vyas, P., Huntley, E., Kissick, K., Belkacemi, M., and Malley, J., Cambridge University Press, Cambridge, UK and New York, NY, USA, 896 pp., https://doi.org/10.1017/9781009157988, 2019.

IPCC: Climate Change 2021: The Physical Science Basis, in: Contribution of Working Group I to the Sixth Assessment Report of the Intergovernmental Panel on Climate Change, edited by: Masson-Delmotte, V., Zhai, P., Pirani, A., Connors, S. L., Péan, C., Berger, S., Caud, N., Chen, Y., Goldfarb, L., Gomis, M. I., Huang, M., Leitzell, K., Lonnoy, E., Matthews, J. B. R., Maycock, T. K., Waterfield, T., Yelekçi, O., Yu, R., and Zhou, B., Cambridge University Press, Cambridge, UK and New York, NY, USA, 2391 pp., https://doi.org/10.1017/9781009157896, 2021.

Ivanov, D. G., Avilov, V. K., and Kurbatova, Y. A.: CO_2 fluxes at south taiga bog in the European part of Russia in summer, Contemp. Probl. Ecol., 10, 97–104, https://doi.org/10.1134/S1995425517020056, 2017.

Ivanov, D. G., Kotlov, I. P., Minayeva, T. Y., and Kurbatova, J. A.: Estimation of carbon dioxide fluxes on a ridge-hollow bog complex using a high resolution orthophotoplan, Nat. Conserv. Res., 6, 16–28, https://doi.org/10.24189/ncr.2021.020, 2021.

Karpov, V. G. (Ed.): Spruce forests of the territory, in: Regulation of factors of spruce forest ecosystems, edited by: Nauka, Leningrad, USSR, 7–31, 1983.

Kljun, N., Calanca, P., Rotach, M. W., and Schmid, H. P.: A simple parameterisation for flux footprint predictions, Bound.-Lay. Meteorol., 112, 503–523, https://doi.org/10.1023/B:BOUN.0000030653.71031.96, 2004.

Koehler, A. K., Sottocornola, M., and Kiely, G.: How strong is the current carbon sequestration of an Atlantic blanket bog?, Global Change Biol., 17, 309–319, https://doi.org/10.1111/j.1365-2486.2010.02180.x, 2011.

Kolle, O. and Rebmann, C.: EddySoft – Documentation of a Software Package to Aquire and Process Eddy Covariance Data, Technical Report 10, Max-Planck-Institut für Biogeochemie, Jena, Germany, 85 pp., https://www.db-thueringen.de/servlets/MCRFileNodeServlet/dbt_derivate_00020684/tech_report10.pdf (last access: 11 March 2022), 2007.

Kurbatova, J., Arneth, A., Vygodskaya, N. N., Kolle, O., Varlargin, A. V., Milyukova, I. M., Tchebakova, N. M., Schulze, E.-D., and Lloyd, J.: Comparative ecosystem–atmosphere exchange of energy and mass in a European Russian and a central Siberian bog I. Interseasonal and interannual variability of energy and latent heat fluxes during the snowfree period, Tellus B, 54, 497–513, https://doi.org/10.3402/tellusb.v54i5.16683, 2002.

Kurbatova, J., Li, C., Varlagin, A., Xiao, X., and Vygodskaya, N.: Modeling carbon dynamics in two adjacent spruce forests with different soil conditions in Russia, Biogeosciences, 5, 969–980, https://doi.org/10.5194/bg-5-969-2008, 2008.

Kurbatova, J., Tatarinov, F., Molchanov, A., Varlagin, A., Avilov, V., Kozlov, D., Ivanov, D., and Valentini, R.: Partitioning of ecosystem respiration in a paludified shallow-peat spruce forest in the southern taiga of European Russia, Environ. Res. Lett., 8, 045028, https://doi.org/10.1088/1748-9326/8/4/045028, 2013.

Kuricheva, O., Mamkin, V., Sandlersky, R., Puzachenko, J., Varlagin, A., and Kurbatova, J.: Radiative entropy production along the paludification gradient in the southern taiga, Entropy, 19, 43, https://doi.org/10.3390/e19010043, 2017.

Lafleur, B., Fenton, N. J., and Bergeron, Y.: Forecasting the development of boreal paludified forests in response to climate change: a case study using Ontario ecosite classification, Forest Ecosyst., 2, 1–11, https://doi.org/10.1186/s40663-015-0027-6, 2015.

Lafleur, P. M., Griffis, T. J., and Rouse, W. R.: Interannual variability in net ecosystem CO_2 exchange at the arctic treeline, Arct. Antarct. Alp. Res., 33, 149–157, https://doi.org/10.1080/15230430.2001.12003417, 2001.

Lafleur, P. M., Moore, T. R., Roulet, N. T., and Frolking, S.: Ecosystem respiration in a cool temperate bog depends on peat temperature but not water table, Ecosystems, 8, 619–629, https://doi.org/10.1007/s10021-003-0131-2, 2005.

Lavoie, M., Paré, D., and Bergeron, Y.: Impact of global change and forest management on carbon sequestration in northern forested peatlands, Environ. Rev., 13, 199–240, https://doi.org/10.1139/a05-014, 2005.

Lindroth, A., Lund, M., Nilsson, M., Aurela, M., Christensen, T. R., Laurila, T., Rinne, J., Riutta, T., Sagerfors, J., Ström, L.,

Tuovinen, J.-P., and Vesala, T.: Environmental controls on the CO_2 exchange in north European mires, Tellus B, 59, 812–825, https://doi.org/10.1111/j.1600-0889.2007.00310.x, 2007.

Lohila, A., Minkkinen, K., Aurela, M., Tuovinen, J.-P., Penttilä, T., Ojanen, P., and Laurila, T.: Greenhouse gas flux measurements in a forestry-drained peatland indicate a large carbon sink, Biogeosciences, 8, 3203–3218, https://doi.org/10.5194/bg-8-3203-2011, 2011.

Loisel, J., Gallego-Sala, A. V., Amesbury, M. J., Magnan, G., Anshari, G., Beilman, D. W., Benavides, J. C., Blewett, J., Camill, P., Charman, D. J., Chawchai, S., Hedgpeth, A., Kleinen, T., Korhola, A., Large, D., Mansilla, C. A., Müller, J., van Bellen, S., West, J. B., Yu, Z., Bubier, J. L., Garneau, M., Moore, T., Sannel, A. B. K., Page, S., Väliranta, M., Bechtold, M., Brovkin, V., Cole, L. E. S., Chanton, J. P., Christensen, T. R., Davies, M. A., De Vleeschouwer, F., Finkelstein, S. A., Frolking, S., Gałka, M., Gandois, L., Girkin, N., Harris, L. I., Heinemeyer, A., Hoyt, A. M., Jones, M. C., Joos, F., Juutinen, S., Kaiser, K., Lacourse, T., Lamentowicz, M., Larmola, T., Leifeld, J., Lohila, A., Milner, A. M., Minkkinen, K., Moss, P., Naafs, B. D. A., Nichols, J., O'Donnell, J., Payne, R., Philben, M., Piilo, S., Quillet, A., Ratnayake, A. S., Roland, T. P., Sjögersten, S., Sonnentag, O., Swindles, G. T., Swinnen, W., Talbot, J., Treat, C., Valach, A. C., and Wu, J.: Expert assessment of future vulnerability of the global peatland carbon sink, Nat. Clim. Change, 11, 70–77, https://doi.org/10.1038/s41558-020-00944-0, 2021.

Lund, M., Lindroth, A., Christensen, T. R., and Stroem, L.: Annual CO_2 balance of a temperate bog, Tellus B, 59, 804–811, https://doi.org/10.1111/j.1600-0889.2007.00303.x, 2007.

Lund, M., Christensen, T. R., Lindroth, A., and Schubert, P.: Effects of drought conditions on the carbon dioxide dynamics in a temperate peatland, Environ. Res. Lett., 7, 045704, https://doi.org/10.1088/1748-9326/7/4/045704, 2012.

Mamkin, V., Kurbatova, J., Avilov, V., Ivanov, D., Kuricheva, O., Varlagin, A., Yaseneva, I., and Olchev, A.: Energy and CO_2 exchange in an undisturbed spruce forest and clear-cut in the Southern Taiga, Agr. Forest Meteorol., 265, 252–268, https://doi.org/10.1016/j.agrformet.2018.11.018, 2019.

Martikainen, P. J., Nykänen, H., Alm, J., and Silvola, J.: Change in fluxes of carbon dioxide, methane and nitrous oxide due to forest drainage of mire sites of different trophy, Plant Soil, 168, 571–577, https://doi.org/10.1007/BF00029370, 1995.

Matthews, B., Mayer, M., Katzensteiner, K., Godbold, D. L., and Schume, H.: Turbulent energy and carbon dioxide exchange along an early-successional windthrow chronosequence in the European Alps, Agr. Foret Meteorol., 232, 576–594, https://doi.org/10.1016/j.agrformet.2016.10.011, 2017.

Mauder, M. and Foken, T.: Impact of post-field data processing on eddy covariance flux estimates and energy balance closure, Meteorol. Z., 15, 597–610, https://doi.org/10.1127/0941-2948/2006/0167, 2006.

Mauder, M., Cuntz, M., Drüe, C., Graf, A., Rebmann, C., Schmid, H. P., Schmidt, M., and Steinbrecher, R.: A strategy for quality and uncertainty assessment of long-term eddy-covariance measurements, Agr. Forest Meteorol., 169, 122–135, https://doi.org/10.1016/j.agrformet.2012.09.006, 2013.

Milyukova, I. M., Kolle, O., Varlagin, A. V., Vygodskaya, N. N., Schulze, E. D., and Lloyd, J.: Carbon balance of a southern taiga spruce stand in European Russia, Tellus B, 54, 429–442, https://doi.org/10.3402/tellusb.v54i5.16679, 2002.

Minkkinen, K., Ojanen, P., Penttilä, T., Aurela, M., Laurila, T., Tuovinen, J.-P., and Lohila, A.: Persistent carbon sink at a boreal drained bog forest, Biogeosciences, 15, 3603–3624, https://doi.org/10.5194/bg-15-3603-2018, 2018.

Moore, P. D.: The future of cool temperate bogs, Environ. Conserv., 29, 3–20, https://doi.org/10.1017/S0376892902000024, 2002.

Mueller, B., Hauser, M., Iles, C., Haque Rimi, R., Zwiers, F. W., and Wan, H.: Lengthening of the growing season in wheat and maize producing regions, Weather Clim. Extrem., 9, 47–56, https://doi.org/10.1016/j.wace.2015.04.001, 2015.

Novenko, E. Y. and Olchev, A. V.: Early Holocene vegetation and climate dynamics in the central part of the East European Plain (Russia), Quatern. Int., 388, 12–22, https://doi.org/10.1016/j.quaint.2015.01.027, 2015.

Park, S. B., Knohl, A., Migliavacca, M., Thum, T., Vesala, T., Peltola, O., Mammarella, I., Prokushkin, A., Kolle, O., Lavrič, J., Park, S. S., and Heimann, M.: Temperature Control of Spring CO_2 Fluxes at a Coniferous Forest and a Peat Bog in Central Siberia, Atmosphere, 12, 984, https://doi.org/10.3390/atmos12080984, 2021.

Parmentier, F. J. W., Van der Molen, M. K., De Jeu, R. A. M., Hendriks, D. M. D., and Dolman, A. J.: CO_2 fluxes and evaporation on a peatland in the Netherlands appear not affected by water table fluctuations, Agr. Forest Meteorol., 149, 1201–1208, https://doi.org/10.1016/j.agrformet.2008.11.007, 2009.

Pavelka, M., Acosta, M., Marek, M. V., Kutsch, W., and Janous, D.: Dependence of the Q_{10} values on the depth of the soil temperature measuring point, Plant Soil, 292, 171–179, https://doi.org/10.1007/s11104-007-9213-9, 2007.

Peel, M. C., Finlayson, B. L., and McMahon, T. A.: Updated world map of the Köppen–Geiger climate classification, Hydrol. Earth Syst. Sci., 11, 1633–1644, https://doi.org/10.5194/hess-11-1633-2007, 2007.

Petrescu, A. M. R., Lohila, A., Tuovinen, J. P., Baldocchi, D. D., Desai, A. R., Roulet, N. T., Vesala, T., Dolman, A. J., Oechel, W. C., Marcolla, B., Friborg, T., Rinne, J., Matthes, J. H., Merbold, L., Meijide, A., Kiely, G., Sottocornola, M., Sachs, T., Zona, D., Varlagin, A., Lai, D. Y. F., Veenendaal, E., Parmentier, F.-J. W., Skiba, U., Lund, M., Hensen, A., van Huissteden, J., Flanagan, L. B., Shurpali, N. J., Grünwald, T., Humphreys, E. R., Jackowicz-Korczyński, M., Aurela, M. A., Laurila, T., Grüning, C., Corradi, C. A. R., Schrier-Uijl, A. P., Christensen, T. R., Tamstorf, M. P., Mastepanov, M., Martikainen, P. J., Verma, S. B., Bernhofer, C., and Cescatti, A.: The uncertain climate footprint of wetlands under human pressure, P. Natl. Acad. Sci. USA, 112, 4594–4599, https://doi.org/10.1073/pnas.1416267112, 2015.

Piao, S., Ciais, P., Friedlingstein, P., Peylin, P., Reichstein, M., Luyssaert, S., Margolis, H., Fang, J., Barr, A., Chen, A., Grelle, A., Hollinger, D. Y., Laurila, T., Lindroth, A., Richardson, A. D., and Vesala, T.: Net carbon dioxide losses of northern ecosystems in response to autumn warming, Nature, 451, 49–52, https://doi.org/10.1038/nature06444, 2008.

Puzachenko, Y. G., Kotlov, L. P., and Sandlerskiy, R. B.: Analysis of changes of land cover using multispectral remote sensing information in the central forest reserve, Izv. Geogr., 3, 5–18, https://doi.org/10.15356/0373-2444-2014-3-5-18, 2014.

Qiu, C., Zhu, D., Ciais, P., Guenet, B., and Peng, S.: The role of northern peatlands in the global carbon cycle for the 21st century, Global Ecol. Biogeogr., 29, 956–973, https://doi.org/10.1111/geb.13081, 2020.

RIHMI-WDC database: Baseline Climatological Data Sets, http://aisori-m.meteo.ru, last access: 11 March 2022.

Roshydromet: Second Roshydromet Assessment Report on Climate Change and its Consequences in the Russian Federation. General summary, Roshydromet, Moscow, 56 pp., http://downloads.igce.ru/publications/OD_2_2014/v2014/pdf/resume_ob_eng.pdf (last access: 11 March 2022), 2014.

Roulet, N. T., Lafleur, P. M., Richard, P. J., Moore, T. R., Humphreys, E. R., and Bubier, J. I. L. L.: Contemporary carbon balance and late Holocene carbon accumulation in a northern peatland, Global Change Biol., 13, 397–411, https://doi.org/10.1111/j.1365-2486.2006.01292.x, 2007.

Schulze, E. D., Vygodskaya, N. N., Tchebakova, N. M., Czimczik, C. I., Kozlov, D. N., Lloyd, J., Sidorov, K. N., Varlagin, A. V., and Wirth, C.: The Eurosiberian transect: an introduction to the experimental region, Tellus B, 54, 421–428, https://doi.org/10.3402/tellusb.v54i5.16678, 2002.

Sulman, B. N., Desai, A. R., Cook, B. D., Saliendra, N., and Mackay, D. S.: Contrasting carbon dioxide fluxes between a drying shrub wetland in Northern Wisconsin, USA, and nearby forests, Biogeosciences, 6, 1115–1126, https://doi.org/10.5194/bg-6-1115-2009, 2009.

Sulman, B. N., Desai, A. R., Saliendra, N. Z., Lafleur, P. M., Flanagan, L. B., Sonnentag, O., Mackay D. S., Barr, A. G. van der Kamp, G.: CO$_2$ fluxes at northern fens and bogs have opposite responses to inter-annual fluctuations in water table, Geophys. Res. Lett., 37, L19702, https://doi.org/10.1029/2010GL044018, 2010.

Syed, K. H., Flanagan, L. B., Carlson, P. J., Glenn, A. J., and Van Gaalen, K. E.: Environmental control of net ecosystem CO$_2$ exchange in a treed, moderately rich fen in northern Alberta, Agr. Forest Meteorol., 140, 97–114, https://doi.org/10.1016/j.agrformet.2006.03.022, 2006.

Tanja, S., Berninger, F., Vesala, T., Markkanen, T., Hari, P., Mäkelä, A., Ilvesniemi, H., Hänninen, H., Nikinmaa, E., Huttula, T., Laurila, T., Aurela, M., Grelle, A., Lindroth, A., Arneth, A., Shibistova, O., and Lloyd, J.: Air temperature triggers the recovery of evergreen boreal forest photosynthesis in spring, Global Change Biol., 9, 1410–1426, https://doi.org/10.1046/j.1365-2486.2003.00597.x, 2003.

Tchebakova, N. M., Vygodskaya, N. N., Arneth, A., Marchesini, L. B., Kurbatova, Y. A., Parfenova, E. I., Valentini, R., Verkhovets, S. V., Vaganov, E. A., and Schulze, E. D.: Energy and mass exchange and the productivity of main Siberian ecosystems (from Eddy covariance measurements). 2. carbon exchange and productivity, Biol. Bull., 42, 579–588, https://doi.org/10.1134/S1062359015660024, 2015.

Ueyama, M., Iwata, H., and Harazono, Y.: Autumn warming reduces the CO$_2$ sink of a black spruce forest in interior Alaska based on a nine-year eddy covariance measurement, Global Change Biol., 20, 1161–1173, https://doi.org/10.1111/gcb.12434, 2014.

Urban SIS: D4.3 Indicators for urban assessments, C3S_441 Lot3 Urban SIS, D4.3, Swedish Meteorological and Hydrological Institute, 55 pp., https://urbansis.eu/wp-content/uploads/2020/03/D4.3_UrbanSIS_Indicators_for_urban_assessments_rev.pdf (last access: 11 March 2022), 2018.

Varlagin, A.: RU-Fyo fluxes, European Fluxes Database Cluster, Fluxdata [data set], http://www.europe-fluxdata.eu/home/site-details?id=RU-Fyo, last access: 11 March 2022.

Vompersky, S. E., Sirin, A. A., Sal'nikov, A. A., Tsyganova, O. P., and Valyaeva, N. A.: Estimation of forest cover extent over peatlands and paludified shallow-peat lands in Russia, Contemp. Probl. Ecol., 4, 734–741, https://doi.org/10.1134/S1995425511070058, 2011.

Vygodskaya, N. N., Schulze, E. D., Tchebakova, N. M., Karpachevskii, L. O., Kozlov, D., Sidorov, K. N., Panfyorov, M. I., Abrazko, M. A., Shaposhnikov, E. S., Solnzeva, O. N., Minaeva, T. Y., Jeltuchin, A. S., Wirth, C., and Pugachevskii, A. V.: Climatic control of stand thinning in unmanaged spruce forests of the southern taiga in European Russia, Tellus B, 54, 443–461, https://doi.org/10.3402/tellusb.v54i5.16680, 2002.

Walker, A. P., Carter, K. R., Gu, L., Hanson, P. J., Malhotra, A., Norby, R. J., Sebestyen, S. D., Wullschleger, S. D., and Weston, D. J.: Biophysical drivers of seasonal variability in Sphagnum gross primary production in a northern temperate bog, J. Geophys. Res.-Biogeo., 122, 1078–1097, https://doi.org/10.1002/2016JG003711, 2017.

Weedon, J. T., Aerts, R., Kowalchuk, G. A., van Logtestijn, R., Andringa, D., and van Bodegom, P. M.: Temperature sensitivity of peatland C and N cycling: does substrate supply play a role?, Soil Biol. Biochem., 61, 109–120, https://doi.org/10.1016/j.soilbio.2013.02.019, 2013.

Welp, L. R., Randerson, J. T., and Liu, H. P.: The sensitivity of carbon fluxes to spring warming and summer drought depends on plant functional type in boreal forest ecosystems, Agr. Forest Meteorol., 147, 172–185, https://doi.org/10.1016/j.agrformet.2007.07.010, 2007.

Wieder, R. K. and Vitt, D. H. (Eds.): Boreal peatland ecosystems, in: Vol. 188, Springer Science & Business Media, 436 pp., https://doi.org/10.1007/978-3-540-31913-9_1, 2006.

Willmott, C. J. and Feddema, J. J.: A more rational climatic moisture index, Profess. Geogr., 44, 84–88, https://doi.org/10.1111/j.0033-0124.1992.00084.x, 1992.

Wutzler, T., Lucas-Moffat, A., Migliavacca, M., Knauer, J., Sickel, K., Šigut, L., Menzer, O., and Reichstein, M.: Basic and extensible post-processing of eddy covariance flux data with REddyProc, Biogeosciences, 15, 5015–5030, https://doi.org/10.5194/bg-15-5015-2018, 2018.

Yu, Z. C.: Northern peatland carbon stocks and dynamics: a review, Biogeosciences, 9, 4071–4085, https://doi.org/10.5194/bg-9-4071-2012, 2012.

Zagirova, S. V., Mikhailov, O. A., and Schneider, J.: Carbon dioxide, heat and water vapor exchange in the boreal spruce and peatland ecosystems, Theor. Appl. Ecol., 3, 12–20, https://doi.org/10.25750/1995-4301-2019-3-012-020, 2019.

Zięba, A. and Ramza, P.: Standard deviation of the mean of autocorrelated observations estimated with the use of the autocorrelation function estimated from the data, Metrol. Meas. Syst., 18, 529–542, 2011.